Plasmodium falciparum subtilisin-like ookinete protein SOPT plays an important and conserved role during ookinete infection of the Anopheles stephensi midgut

Armistead, J.S.; Jennison, C.; O'Neill, M.T.; Lopaticki, S.; Liehl, P.; Hanson, K.K.; ... ; Boddey, J.A.

Plasmodium falciparum **subtilisin-like ookinete protein SOPT plays an important and conserved role during ookinete infection of the** ***Anopheles stephensi*** **midgut**

Jennifer S. Armistead[1,2], Charlie Jennison[1,2], Matthew T. O'Neill[1], Sash Lopaticki[1], Peter Liehl[3], Kirsten K. Hanson[3], Takeshi Annoura[4], Pravin Rajasekaran[1,2], Sara M. Erickson[1,2], Christopher J. Tonkin[1,2], Shahid M. Khan[4], Maria M. Mota[3] and Justin A. Boddey[1,2,*]

[1] The Walter and Eliza Hall Institute of Medical Research, Parkville 3052, Victoria, Australia.

[2] Department of Medical Biology, The University of Melbourne, Parkville 3052, Victoria, Australia.

[3] Instituto de Medicina Molecular, Faculdade de Medicina Universidade de Lisboa, 1649-028 Lisbon, Portugal.

[4] Leiden Malaria Research Group, Parasitology, Leiden University Medical Centre, 2333ZA Leiden, the Netherlands.

*Correspondence and requests for materials should be addressed to J.A.B (boddey@wehi.edu.au)

Running title: SOPT facilitates ookinete infection of mosquitoes

Key words*:* malaria*,* mosquito, transmission, traversal, invasion

Summary

Transmission of the malaria parasite *Plasmodium falciparum* involves infection of *Anopheles* mosquitoes. Here we characterize SOPT, a protein expressed in *P. falciparum* ookinetes that facilitates infection of the mosquito midgut. SOPT was identified on the basis that it contains a signal peptide, a PEXEL-like sequence and is expressed in asexual, ookinete and sporozoite stages, suggesting it is involved in infecting the human or mosquito host. SOPT is predicted to contain a subtilisin-like fold with a non-canonical catalytic triad and is orthologous to *P. berghei* PIMMS2. Localization studies reveal that SOPT is not exported to the erythrocyte but is expressed in ookinetes at the parasite periphery. *SOPT*-deficient parasites develop normally through the asexual and sexual stages and produce equivalent numbers of ookinetes to NF54 controls, however, they form fewer oocysts and sporozoites in mosquitoes. SOPT-deficient parasites were also unable to activate the immune-responsive midgut invasion marker *SRPN6* after mosquito uptake, suggesting they are defective for entry into the midgut. Disruption of *SOPT* in *P. berghei* (PIMMS2) did not affect other lifecycle stages or ookinete development but again resulted in fewer oocysts and sporozoites in mosquitoes. Collectively, this study shows that SOPT/PIMMS2 plays a conserved role in ookinetes of different *Plasmodium* species.

Introduction

Malaria continues to be an enormous global health burden with an estimated 220 million cases and 630,000 deaths occurring in 2015 (Gething *et al.*, 2016). *Plasmodium* parasites cause malaria and are maintained between humans and *Anopheles* mosquitoes in a complex life cycle that requires the parasite to invade different cell types in both hosts. Following mosquito ingestion of an infectious blood meal, male and female gametocytes differentiate into gametes, which fuse during fertilization to form a diploid zygote, later developing into a motile ookinete. The ookinete must make its way from the midgut lumen to the midgut periphery (Angrisano *et al.*, 2012), where it attaches to and traverses the midgut epithelium, notably in the absence of a parasitophorous vacuole membrane, in order to arrive at the basal lamina where it forms an oocyst, undergoing sporogony to generate thousands of sporozoites. Upon rupture of mature oocysts, sporozoites are released into the hemocoel where they migrate to and invade the salivary glands, rendering the mosquito infectious. Following injection into the skin during a subsequent blood meal, sporozoites travel to the liver sinusoids, where they must traverse an endothelial barrier before traversing and invading hepatocytes. Within hepatocytes, parasites form a parasitophorous vacuole and undergo schizogony, eventually rupturing and releasing erythrocyte-invasive merozoites into the bloodstream, initiating the symptomatic phase of the life cycle known as malaria.

Invasion and traversal of mosquito midgut epithelial cells and human hepatocytes by *Plasmodium* ookinetes and sporozoites, respectively, represent major population bottlenecks in the parasite life cycle (Sinden, 2010). Thus, the specific molecular host-parasite interactions that facilitate these processes represent promising targets for the development of novel interventions to interrupt transmission. Several key ookinete proteins have been implicated in midgut invasion. P25 and P28 protect the ookinete from the hostile environment of the midgut (Tomas *et al.*, 2001), and along with enolase (Ghosh *et al.*, 2011) and CTRP (circumsporozoite and TRAP-related protein) (Dessens *et al.*,

1999, Yuda *et al.*, 1999) are thought to facilitate initial interactions with the epithelial cell surface. PPL3 (Kadota *et al.*, 2004) and 5 (*Plasmodium* perforin like proteins 3 and 5) (Kadota *et al.*, 2004, Ecker *et al.*, 2008), PSOP (putative secreted ookinete protein) 2 and 7 (Ecker *et al.*, 2008), and SOAP (secreted ookinete adhesive protein) (Dessens *et al.*, 2003), WARP (von Willebrand factor A domain-related protein) (Yuda *et al.*, 2001), and LIMP (Santos *et al.*, 2017) have functions in invasive motility, while SUB2 (subtilisin-like protease 2) (Han *et al.*, 2000) and CelTOS (cell traversal protein for ookinetes and sporozoites) (Kariu *et al.*, 2006, Steel *et al.*, 2018) have been identified to play a role in traversal of the midgut epithelium and oocyst survival.

Here, we characterize SOPT (subtilisin-like ookinete protein important for transmission), which is expressed in *P. falciparum* ookinetes near the parasite periphery. Genetic disruption of *SOPT* in *P. falciparum* significantly reduces oocyst development and *SRPN6* (*serpin 6*) gene expression in *An. stephensi* midguts, suggesting the protein facilitates initial entry of the ookinete into the midgut epithelium prior to cell traversal and subsequent oocyst formation. Disruption of *P. berghei* SOPT (also called PIMMS2; *Plasmodium* invasion of mosquito midgut screen candidate 2) also reduced the number of oocysts and sporozoites in *An. stephensi* mosquitoes, as has also been shown previously (Ukegbu *et al.*, 2017). Therefore, SOPT/PIMMS plays a conserved role in different *Plasmodium* spp. during ookinete infection of the mosquito.

Results

Identification of SOPT in *P. falciparum*.

PF3D7_0507300 (*SOPT*) was identified in a bioinformatic screen using PlasmoDB to search for *P. falciparum* genes that are conserved across the genus and encode an N-terminal signal peptide and putative PEXEL motif (*Plasmodium* export element; (Marti *et al.*, 2004, Hiller *et al.*, 2004), filtered for expression in asexual, ookinete and/or sporozoite stages. *SOPT* was selected for study because mRNA

transcripts had been detected in *P. falciparum* ookinetes and sporozoites (Florens *et al.*, 2002, Lopez-Barragan *et al.*, 2011, Bunnik *et al.*, 2013) in addition to proteomic evidence of expression in merozoites (Florens *et al.*, 2002), suggesting it may contribute to infection of the mosquito or human host.

SOPT and one other gene have a conserved location between *SUB1 (subtilisin 1*; PF3D7_0507500) and *SUB3 (subtilisin 3*; PF3D7_0507200) in different *Plasmodium* species. *SOPT* is predicted to encode an 893 amino acid protein of 107 kDa that contains a signal peptide (SignalP prediction ^{23}FLL↓ KQ^{27}), a PEXEL-like sequence (^{38}RILEE^{42}) and a putative transmembrane helix (position 490-505). A homology model of SOPT revealed a 387 amino acid subtilisin-like fold from the S8 peptidase family, similar to that of SUB1 from *P. falciparum* (Withers-Martinez *et al.*, 2014) (Fig. 1A). The model was sufficient to reveal the conserved positions of putative catalytic residues. However, the catalytic triad in SUB1 (D372, H428 and S606) was absent from SOPT, with only the nucleophile serine present (G172, E247 and S492) (Fig. 1B). In contrast, *P. berghei* SOPT/PIMMS2 possessed a canonical triad with potential to form a charge-relay network typical of subtilisins (D155, H222, S414) (Fig. 1C). A multiple sequence alignment of *Plasmodium* orthologs revealed that catalytic residues were not conserved, with SOPT from *P. malariae*, *P. reichenowi*, *P. yoelii* and *P. chabaudi chabaudi* lacking either the catalytic aspartate and/or histidine residue, like *P. falciparum*, while orthologs in *P. vivax*, *P. ovale*, *P. knowlesi* and *P. gallinaceum* possessed a canonical triad, as in *P. berghei* (Fig. 1C). The putative transmembrane helix internal to SOPT is also predicted in some orthologs; however, it is positioned within 5 amino acids from the nucleophile serine residue, suggesting that the transmembrane helix prediction may be incorrect. No protein domain in the C-terminus of SOPT was identified by computational methods or modelling. Given the divergent catalytic triad across the genus, it is likely that SOPT is a pseudoprotease rather than an active protease in

Plasmodium spp., as is the case for the protein SERA5 (serine rich antigen 5) (Stallmach *et al.*, 2015, Collins *et al.*, 2017).

An alignment of N-termini from different SOPT orthologs revealed a conserved RxLxE sequence with similarity to the PEXEL (Marti *et al.*, 2004, Hiller *et al.*, 2004) (Fig. 1D). The ability for this sequence to direct export to the infected erythrocyte was investigated by generating transgenic *P. falciparum* parasites in which the first 62 residues of SOPT were expressed in-frame with GFP (green fluorescent protein) from the *CRT* (*chloroquine resistance transporter*) gene promoter on episomes in asexual stages (Fig. 1E). The first 62 residues were chosen to provide a spacer of 20 amino acids between the PEXEL-like sequence and GFP, since the tag can block PEXEL function if it is located within 13 residues of the motif (Knuepfer *et al.*, 2005). Immunoblot with anti-GFP antibodies confirmed expression of SOPT_1-62-GFP in blood stage parasites (Fig. 1F). The immunoblot also identified a GFP-only degradation product thought to be produced by digestion of GFP chimeras in the food vacuole (Waller *et al.*, 2000). Immunofluorescence microscopy of live parasites revealed that the chimera was secreted to the parasite periphery, consistent with the parasitophorous vacuole, confirming that the signal peptide was functional, but was not visibly exported (Fig. 1G). The majority of genes encoding exported PEXEL proteins have a two exon structure (Sargeant *et al.*, 2006) whereas *SOPT* consists of a single exon. It has been previously reported that single exon genes that possess PEXEL-like sequences, such as *SOPT*, are not exported (Sargeant *et al.*, 2006). Collectively, these results show that SOPT is a conserved protein in *Plasmodium* species and has a functional signal peptide for entering the secretory pathway but is not exported to the erythrocyte when tagged with GFP.

Generation of SOPT-deficient *P. falciparum*.

To study the function of SOPT in *P. falciparum*, NF54 parasites were generated in which the *SOPT* gene was disrupted by double-crossover homologous recombination (Fig. 2A). Two independent

knockout clones, D4 and E8, were selected with the expected genotype as shown by Southern blot analysis (Fig. 2B). The generation and selection of *SOPT*-deficient parasites demonstrates that this gene is not essential in asexual stages of *P. falciparum*. Since SOPT is expressed in merozoites (Florens *et al.*, 2002), we compared the growth rate of blood stage parasites. The growth rate was not different between Δ*SOPT* mutants and the parent line NF54 (Fig. 2C), indicating that SOPT is not essential for invasion or egress of erythrocytes. Production of gametocytes appeared normal, with no significant differences in stage V gametocytemias observed (Fig. 2D). In summary, the *SOPT* gene is amenable to genetic disruption and its product is not essential in the asexual stage or for gametocytogenesis of *P. falciparum*.

SOPT is expressed in *P. falciparum* ookinetes and localizes at the parasite periphery.

Evidence of *SOPT* gene expression in ookinetes has been detected previously with RNA sequencing (Lopez-Barragan *et al.*, 2011). To study expression and localization at the protein level, an antibody was produced using the SOPT subtilisin-like domain as an antigen. Immunofluorescence microscopy was then performed on ookinetes dissected from *Anopheles stephensi* midguts one-day after blood feeding via SMFAs (standard membrane feeding assays). Expression of SOPT was observed near the periphery of the ookinetes, as evidenced by partial co-localization with the ookinete surface protein Pfs25 (Barr *et al.*, 1991), and a strong signal was observed at the anterior of the parasites (Fig. 2E). In Δ*SOPT* ookinetes, no signal was detected with anti-SOPT antibodies, whilst Pfs25 expression remained detectable (Fig. 2E). This shows that SOPT localizes in *P. falciparum* ookinetes at, or in close proximity to, the plasmalemma.

SOPT facilitates *P. falciparum* infection of the mosquito midgut.

To investigate whether SOPT has an important function in ookinetes, Δ*SOPT* parasites were differentiated to gametocytes and fed to *An. stephensi* mosquitoes. The following day, mosquito midguts were dissected and the number of activated female gametes/zygotes (round forms), partially developed ookinetes (retorts) and mature ookinetes was quantified by microscopy. This showed no deficiency in the ability of Δ*SOPT* parasites to differentiate into gametes/zygotes, retorts or ookinetes compared to NF54 (Fig. 3A). However, when midguts were dissected one-week post mosquito infection, a significant reduction in oocyst numbers was observed for Δ*SOPT* mutants compared to NF54 (Fig. 3B, Supporting Information Table S1). The number of salivary gland sporozoites was also reduced in mosquitoes fed Δ*SOPT* parasites compared to NF54 (Fig. 3C, Supporting Information Table S1), a phenotype that is expected based on the reduction in oocysts. Since genetic disruption of *SOPT* did not affect the numbers of ookinetes developing in mosquitoes, we conclude that SOPT plays a role during infection of the midgut, possibly during traversal of the epithelium or as oocysts develop at the basal lamina.

To distinguish between these two possibilities, parasites were fed to mosquitoes and quantitative PCR was used to measure expression of the immune-responsive invasion marker *SRPN6* (*serpin 6*) in midguts on the following day. *SRPN6* expression is upregulated in midgut epithelial cells in response to intracellular ookinetes and other pathogens (Abraham *et al.*, 2005, Pinto *et al.*, 2008, Smith *et al.*, 2012, Eappen *et al.*, 2013) and its expression can be used as a reporter for parasite invasion of the epithelium *in situ*. Relative to sugar-fed mosquitoes, midguts containing NF54 parasites had increased *SRPN6* expression, as expected, confirming that these parasites could successfully traverse the midgut (Fig. 3D). However, Δ*SOPT* parasites failed to induce the same level of *SRPN6* expression as their NF54 parents (Fig. 3D). Standardizing *SRPN6* expression for ookinete abundance using the *P. falciparum CTRP* gene (Trottein et al., 1995) confirmed that the defect in *SRPN6* activation was not due to any potential differences in ookinete numbers (Fig. S1). Together, this

strongly suggests that *SOPT* mutants are defective for entering the midgut epithelium, which is the first step in traversal.

The function of SOPT is conserved in different *Plasmodium* species.

To evaluate whether SOPT plays a similar role in other *Plasmodium* species, a SOPT/PIMMS2-deficient line was generated in *P. berghei* ANKA constitutively expressing a GFP-luciferase fusion in the cytoplasm (GFP-Luc$_{con}$) (Janse *et al.*, 2006a) by double cross-over homologous recombination (Fig. 4A). Independent PbΔ*SOPT/PIMMS2* clones with the correct genotype were identified by diagnostic PCR (Fig. 4B) and Southern blot analysis (Supporting Information Fig. S1). The mutant clones exhibited blood stage growth rates during the cloning period that were comparable to GFP-Luc$_{con}$ controls (data not shown), consistent with PbSOPT/PIMMS2 being dispensable in blood stages, as observed in *P. falciparum.*

PbSOPT/PIMMS2 mutants were then transmitted to mosquitoes via direct biting on anesthetized mice and on the following day, midguts were dissected and female gametes/zygotes (round forms), retorts and ookinetes were quantified. This showed no defect in ookinete development for PbSOPT/PIMMS2 mutants compared to controls (Fig. 4C). Whilst the average number of ookinetes per mosquito was marginally increased following disruption of *PbSOPT/PIMMS2*, possibly due to variation of gametocyte numbers between mice, the mutants generated fewer oocysts (Fig. 4D, Supporting Information Table S2) and salivary gland sporozoites (Fig. 4E, Supporting Information Table S2) per mosquito compared to GFP-Luc$_{con}$ parent parasites, consistent with an important role during infection of the midgut.

To control for possible variation in *P. berghei* gametocytogenesis between mice, which could influence the number of parasites in mosquito midguts, infected erythrocytes containing gametocytes were cultured *in vitro* to produce ookinetes. This method resulted in the production of approximately

equal numbers of Pb∆*SOPT/PIMMS2* and GFP-Luc$_{con}$ ookinetes (Fig. 5A). These were fed to *An. stephensi* mosquitoes using SMFAs. Despite the equal inoculum, Pb∆*SOPT/PIMMS2* ookinetes produced significantly fewer oocysts per mosquito compared to GFP-Luc$_{con}$ parasites (Fig. 5B, Supporting Information Table S3). Altogether, our results demonstrate that PbSOPT/PIMMS2 is important for *P. berghei* ookinete infection of the mosquito midgut, consistent with a recent report that PIMMS2 is involved in midgut traversal (Ukegbu *et al.*, 2017). The similar loss-of-function phenotypes we observed using both *P. falciparum* and *P. berghei* mutants demonstrates that SOPT/PIMMS2 plays a conserved function in these two species during mosquito infection, likely at the step of midgut invasion. As noted above, PfSOPT and PbSOPT/PIMMS2 bear different catalytic triads, supporting the hypothesis that these proteins could be pseudoenzymes.

PbSOPT/PIMMS2 is dispensable for sporozoite infectivity and establishing patency.

The production of oocysts and sporozoites in mosquitoes containing Pb∆*SOPT/PIMMS2* parasites, albeit at low numbers, provided the opportunity to examine a possible role of SOPT in sporozoite infectivity and subsequent development of liver stages. Despite Pb∆*SOPT/PIMMS2* producing low numbers of salivary gland sporozoites, we were able to obtain sufficient sporozoites to infect mice. Mice were intravenously infected with 10,000 sporozoites of PbGFP-Luc$_{con}$ or Pb∆*SOPT/PIMMS2* and parasite liver load was quantified two days post-infection by RTq-PCR. No significant defect in parasite liver load was observed (Fig. 5C), demonstrating that PbSOPT/PIMMS2 is not essential for sporozoite infectivity or liver stage development *in vivo*. Next, we determined time to blood stage patency in mice infected with 10,000 sporozoites. The mean time to patency was 4.6 ± 0.2 days for Pb∆*SOPT/PIMMS2* and 4.4 ± 0.2 days for PbGFP-Luc$_{con}$ ($P>0.9999$; two independent experiments) indicating no significant delay between strains. Once patency had been established, no

difference in parasitemia was observed for a period of 5 days (Fig. 5D), in agreement with our results that SOPT/PIMMS2 is dispensable during erythrocyte infection. Collectively, these results demonstrate that PbSOPT/PIMMS2 is not required for sporozoite infectivity in mouse livers, for transitioning from the liver to the blood stage, or for *in vivo* growth in erythrocytes following sporozoite inoculation.

Discussion

The life cycle of the malaria parasite requires invasion of different cell types in both the human host and mosquito vector. Host-parasite molecular interactions that facilitate invasion of the mosquito midgut epithelium or human hepatocytes by *Plasmodium* ookinetes or sporozoites, respectively, are promising targets for developing transmission-blocking interventions. In this study, we have shown that SOPT facilitates transmission of *P. falciparum* and *P. berghei* ookinetes to mosquitoes. Our experiments using the *P. falciparum-An. stephensi* laboratory model suggest that SOPT functions during the initial entry step of midgut traversal. A previous study with *P. berghei-An. gambiae* infections showed that loss of PIMMS2 (PbSOPT) resulted in a traversal defect, determined by a reduction in ookinete melanization at the basal lamina (Ukegbu *et al.*, 2017). While we cannot exclude that SOPT is involved in ookinete locomotion, which is technically challenging to measure with *P. falciparum* ookinetes because they are difficult to culture *in vitro*, disruption of *PIMMS2* (*PbSOPT*) had no effect on *P. berghei* ookinete gliding motility (Ukegbu *et al.*, 2017). Collectively, both this study and that of Ukegbu *et al.*, (2017) come to a similar conclusion that SOPT and PIMMS2 are involved in ookinete invasion of the mosquito midgut epithelium. While also apparently expressed/transcribed in merozoites and sporozoites (Florens *et al.*, 2002, Lopez-Barragan *et al.*, 2011, Bunnik *et al.*, 2013), genetic disruption of SOPT/PIMMS2 had no effect on asexual growth, gametocytogenesis, sporozoite infectivity or establishment of patent infections (Ukegbu *et al.*, 2017 and this study).

The precise steps of mosquito midgut invasion are not fully understood, but numerous parasite proteins have been implicated. SOPT/PIMMS2 clearly plays an important role, although infection is not completely blocked as it is following disruption of *CTRP* (Dessens *et al.*, 1999, Yuda *et al.*, 1999, Templeton *et al.*, 2000). This partial block in infectivity has also been observed in other mutants lacking expression of surface or secreted proteins of ookinetes (Han *et al.*, 2000, Tomas *et al.*, 2001, Kariu *et al.*, 2006, Ghosh *et al.*, 2011). In one such instance it was postulated that P25/P28 double knockout parasites may take an intercellular (between two cells) route to traverse the midgut epithelium (Danielli *et al.*, 2005). It is possible that some *SOPT/PIMMS2*-deficient ookinetes may have crossed the epithelium via an alternative, extracellular route, however further studies are needed to confirm or disprove this.

SOPT represents a fourth subtilisin-like protein in *Plasmodium*, along with three previously characterized proteases, SUB1, 2, and 3, which are highly expressed in late asexual blood stages (Le Roch et al., 2003). SUB1 processing of parasitophorous vacuolar proteins, including the SERA (serine-rich antigen) proteins (Arastu-Kapur *et al.*, 2008, Ruecker *et al.*, 2012) and the MSP1 (merozoite surface protein 1) complex (Harris *et al.*, 2005b, Child *et al.*, 2010, Silmon de Monerri *et al.*, 2011), is critical to merozoite egress and invasion. SUB1 is also essential for development of liver stage schizonts and egress of merozoites from hepatocytes (Suarez *et al.*, 2013, Tawk *et al.*, 2013). SUB2 similarly plays a role in merozoite invasion through processing of MSP1, AMA1 (apical membrane antigen 1), and PTRAMP (*Plasmodium* thrombospondin related apical merozoite protein) (Barale *et al.*, 1999, Fleck *et al.*, 2003, Dutta *et al.*, 2005, Harris *et al.*, 2005a, Howell *et al.*, 2005, Green *et al.*, 2006). SUB2 is additionally expressed within osmophilic bodies of gametocytes (Suarez-Cortes *et al.*, 2016), and is secreted into the cytoplasm of invaded midgut epithelial cells, where it may function to modify the cytoskeletal network (Han *et al.*, 2000). While SUB2 is essential for *P. berghei* merozoite invasion of red blood cells (Uzureau *et al.*, 2004, Bushell *et al.*, 2017), its exact function during

invasion or traversal of the mosquito midgut remains unclear. SUB2 and SOPT/PIMMS2 are apparently co-expressed in *P. berghei* ookinetes, although it is unknown if the two proteins co-localize or interact at any point during midgut invasion or traversal. The possibility that they may function cooperatively to promote midgut colonization should be explored further. PfSUB3 has been confirmed to possess serine protease activity and appears to play a role in evasion of host immune responses through interactions with a *P. falciparum* PRF (profilin) (Alam *et al.*, 2012).

Subtilisin-like proteases, including *Plasmodium* SUB1, 2, and 3, are typically characterized by a catalytic triad of Asp, His, and Ser residues and an α/β protein scaffold (Siezen & Leunissen, 1997). SOPT exhibits subtilisin-like structural features, however one or more catalytic residues are absent among many *Plasmodium* orthologs. While PbSOPT/PIMMS2 does possess the canonical catalytic triad, mutagenesis of the conserved Asp-His-Ser residues did not result in a loss-of-function phenotype as severe as that seen in knockout parasites (Ukegbu *et al.*, 2017). Taken together, this indicates that the catalytic triad is not critical to the function of SOPT/PIMMS2 and suggest that it has a non-enzymatic role in *Plasmodium* ookinete entry into the mosquito midgut epithelium, which is the first step of the traversal process. However, additional biochemical and structural analyses are needed for confirmation that SOPT is indeed a pseudoprotease, such as those reported previously for SERA 5 (Stallmach *et al.*, 2015).

Catalytically deficient variants are found in all major enzyme families and are widespread throughout evolution. The function of many is unknown, but for a number an important role in various cellular functions have been shown (Eyers & Murphy, 2016), including regulation of active enzyme counterparts, signaling, substrate trafficking, and in many pathogens also modulation of host immune responses (Reynolds & Fischer, 2015). *Plasmodium* pseudoenzymes include CyRPA (cysteine-rich protective antigen), a pseudosialidase that forms a multi-protein complex that is essential for merozoite invasion of erythrocytes (Chen *et al.*, 2017, Favuzza *et al.*, 2017), and SERA5, a non-active papain-like

protease thought to regulate the function of SERA6 in merozoite egress by controlling access to its substrates (Stallmach *et al.*, 2015). A non-catalytic ATP-dependent caseinolytic protease, ClP-R, has also recently been identified within the parasite apicoplast, although its function is currently unknown (El Bakkouri *et al.*, 2013).

In conclusion, SOPT/PIMMS2 is a conserved protein in *Plasmodium* that likely facilitates ookinete entry into the mosquito midgut to initiate traversal. Although structurally similar to other *Plasmodium* subtilisin-like proteins, bioinformatics and homology modelling suggest SOPT and its orthologs could be pseudoenzymes with an as-yet unknown direct function. This study indicates that SOPT is important among the complex, hierarchical series of molecular interactions between the *Plasmodium* ookinete and the mosquito midgut, and as such, the biological function should be explored further.

Experimental procedures

Bioinformatics and homology modelling

Signal peptides were predicted with SignalP 3.0 (Bendtsen *et al.*, 2004) using neural networks (NN) and hidden Markov models (HMM) trained on eukaryotes (http://www.cbs.dtu.dk/services/SignalP-3.0/). Multiple sequence alignments were performed using Clustal Omega (Sievers *et al.*, 2011)(http://www.ebi.ac.uk/Tools/msa/clustalo/). Known domains, motifs and transmembrane helices were predicted using the PROSITE (http://prosite.expasy.org/scanprosite/) (Gattiker *et al.*, 2002) and Phyre2 2.0 (http://www.sbg.bio.ic.ac.uk/phyre2). (Kelley *et al.*, 2015) servers. A homology model for *P. falciparum* SOPT was built using Phyre2 2.0 and the model was overlaid on the structure of *P. falciparum* SUB1 (4LVN) (Withers-Martinez *et al.*, 2014) using The PyMOL Molecular Graphics System.

Parasite maintenance

The asexual stages of *Plasmodium falciparum* strain NF54 were maintained in human type O positive erythrocytes (Australian Red Cross) at 4% hematocrit. RPMI-HEPES media supplemented with 10% serum (7% heat inactivated human serum [Australian Red Cross]; 3% Albumax [Life Technologies]) were used to maintain the parasites at 37 °C in 94% N, 5% CO_2, 1% O_2. Sexual forms of the parasite were generated using the crash method as previously described (Saliba & Jacobs-Lorena, 2013). Gametocytes were maintained in O^+ red blood cells (Australian Red Cross) in RPMI medium supplemented with 25 mM HEPES, 25 mM $NaHCO_3$, 12.5 ug/mL hypoxanthine, 0.2% glucose, and 10% heat-inactivated O^+ human serum (Australian Red Cross), with daily media changes. Gametocyte cultures were harvested 16 to 17 days after initiation and diluted with human O^+ red blood cells and heat-inactivated serum to 0.3% gametocytemia and 50% haematocrit. Infective blood was delivered directly into water-jacketed glass membrane feeders maintained at 37 ºC via a circulating water bath.

Fifty female *An. stephensi* (3-5 d old) mosquitoes were allowed to feed from each feeder for 30 minutes, after which any unfed mosquitoes were collected and discarded. Numbers of sexual stages (gametes/zygotes, retorts, ookinetes), oocysts, and sporozoites per mosquito were determined at 24 h, 8 d, and 14 d post-bloodfeeding, respectively, as described below. Three independent replicate experiments were performed with NF54 and each Δ*SOPT* clone (D4 and E8). The reference line 676m1cl1 of *P. berghei* ANKA strain was used (*Pb*GFP-Luc$_{con}$; see RMgm-29 in www.pberghei.eu). *Pb*GFP-Luc$_{con}$ contains the *gfp-luc* fusion gene under control of the constitutive *eef1α* promoter, integrated into the silent *230p* gene locus (PBANKA_030600); the line does not contain a drug-selectable marker (Janse *et al.*, 2006b).

Transgenic parasites

P. falciparum NF54 was used to generate all transgenic parasites used in this study. To generate the PfSOPT 1-61-GFP parasites synthetic gBlocks® gene fragments were manufactured by Integrated DNA Technologies for the sequence SOPT_1-61. This was cloned into pGlux using XhoI/XmaI. *P. falciparum* transfectants were selected with 5 nM WR99210 (Jacobus Pharmaceuticals). To generate the SOPT knockout construct, 5' and 3' flanks of the locus were cloned into pCC1 using SacII/SpeI (5' flank) and EcoR1/AvrII (3' flank). Primers for amplification of SOPT (PF3D_1147800) 5' and 3' flanks are listed in Table S4. Purified plasmid DNA (80 µg) was transfected into ring stage NF54 and selected using 5 nM WR92210. Lines were cloned by limiting dilution and genotypes assessed by Southern blot using the digoxigenin kit (DIG) from Roche, according to manufacturer's instructions. To generate a *P. berghei* mutant line lacking expression PBANKA_110690*,* we targeted the gene locus for deletion using a linear construct, generated using a 2-step anchor tagging PCR method (Lin *et al.*, 2011). The 5'- and 3' targeting regions of the gene were PCR amplified from genomic DNA using primer pairs 4744/4745 and 4746/4747 (for primer details see Table S4). Primers 4745 and 4747 have

5'-terminal extensions homologous to the *hdhfr* selectable marker cassette. Primers 4744 and 4747 both have a 5'-terminal overhang with an anchor-tag which serves as a primer site in the 2nd PCR reaction. The target fragments from the first PCR reaction were annealed to either side of the selectable marker cassette by PCR with anchor-tag primers 4661 and 4662, resulting in the 2nd PCR product. To remove the 'anchor', the final PCR fragment was digested with *Asp*718 and *Sca*I (primers 4744 and 4747 contained *Asp*718 and *Sca*I restriction enzyme sites, respectively), resulting in construct pL1500. The *hdhfr* selectable marker cassette used in this reaction was digested from pL0040 using restriction enzymes *Xho*I and *Not*I (pL0040 is available from The Leiden Malaria Research Group).

To generate a *P. berghei* mutant line lacking expression of PbSOPT/PIMMS2 (PBANKA_110690), we targeted the gene locus for deletion using a linear construct, generated using a 2-step anchor tagging PCR method (Janse *et al.*, 2006b) (Supplementary Information Fig. 1). The 5'- and 3' targeting regions of the gene were PCR amplified from genomic DNA using primer pairs 4744/4745 and 4746/4747 (for primer details see Table S1). Primers 4745 and 4747 have 5'-terminal extensions homologues to the *hdhfr* selectable marker cassette. Primers 4744 and 4747 both have a 5'-terminal overhang with an anchor-tag which serves as a primer site in the 2nd PCR reaction. The target fragments from the first PCR reaction were annealed to either side of the selectable marker cassette by PCR with anchor-tag primers 4661 and 4662, resulting in the 2nd PCR product. To remove the 'anchor', the final PCR fragment was digested with *Asp*718 and *Sca*I (primers 4744 and 4747 contained *Asp*718 and *Sca*I restriction enzyme sites, respectively), resulting in construct pL1500. The *hdhfr* selectable marker cassette used in this reaction was digested from pL0040 using restriction enzymes *Xho*I and *Not*I (pL0040 is available from The Leiden Malaria Research Group).

Transfection of parasites of the *P. berghei* ANKA reference line *Pb*GFP-Luc$_{con}$ with construct pL1500, selection and cloning of the mutant parasite line was performed as described (Janse *et al.*, 2006b). Correct integration of the DNA constructs was determined by diagnostic PCR and Southern

analysis of chromosomes separated by pulse-field gel (PFG) electrophoresis. Southern blots were hybridized with a probe recognizing the 3'UTR *dhfr/ts* of *P. berghei* ANKA. We obtained three independent clones with the correct genotype and the clones exhibit blood stage growth rates (during the cloning period) that is comparable to wild type *P. berghei* ANKA blood stage parasites, and while only clone 1482cl1 is shown, two knockout clones were used to assess phenotypes across the lifecycle (data not shown).

Asexual blood stage growth assay

Highly synchronous trophozoite stage parasites were diluted to 0.5% parasitemia at 2% hematocrit and this was confirmed by flow cytometry (FACSCalibur; BD) using ethidium bromide (10 μg/ml; BioRad) (Sleebs *et al.*, 2014). Final parasitemia was determined 48 hours later by FACS as above. For each line, triplicate samples of 50,000 cells were counted in each of the three independent experiments. Growth was expressed as fold-change relative to the parasitemia achieved by NF54.

Mosquito infection and analysis of parasite development

Five- to 7-day old female *An. stephensi* mosquitoes were fed a bloodmeal of asynchronous gametocytes at 0.3% stage V gametocytemia by standard membrane feeding assays (SMFAs). Mosquitoes were sugar starved for 16-24 hours before and another 48 hours post bloodmeal to select the bloodfed females from a mixed mosquito population. Surviving mosquitoes were provided sugar cubes and water (via cotton wick) *ad libitum*. At 24 h post-blood feeding, infected midguts were dissected, and contents pooled from 25 mosquitoes. Contents were lysed with 0.5% saponin (w/v) in phosphate buffered saline (PBS), washed three times, and resuspended in 25 μl PBS. 2 μl of each resuspended pellet was spotted onto a glass slide, stained with Giemsa, and round forms (gametes/zygotes), retorts, and ookinetes within the entire spot were quantified by light microscopy to determine the number per

mosquito. At 8 days (*P. falciparum*) or 10 days (*P. berghei*) post-bloodfeeding, midguts were dissected from cold-anesthetized and ethanol-killed mosquitoes and stained with 0.1% mercurochrome (w/v) in water, and oocysts per mosquito enumerated by microscopy. At 14 days (*P. falciparum*) or 21 days (*P. berghei*) days post-bloodfeeding, salivary glands were dissected from individual mosquitoes and homogenized in 40 µl PBS with a pestle to release sporozoites. Following centrifugation at 6,000 x g for 3 min, the supernatant was collected and sporozoites were counted using a Neubauer hemocytometer.

An. stephensi and *P. falciparum* gene expression

Gene expression was analyzed in *An. stephensi* midguts 27 h after SMFA, as described previously (Lopaticki *et al.*, 2017). Briefly, mosquitoes were cold anesthetized, and ethanol killed. Midguts from 25 mosquitoes per group were dissected and frozen immediately on dry ice. RNA was purified using TRI Reagent (Sigma) and complementary DNA (cDNA) prepared using a SensiFast cDNA synthesis kit (Bioline) according to the manufacturers' instructions. RTq-PCR was performed using a LightCycler 480 (Roche) using oligonucleotides listed in Table S4.

Antibody production

PfSOPT (E101 to I350) was expressed as a His-tag recombinant fusion protein, purified by affinity chromatography and used for immunization of two rabbits by Genscript Corp. Serum was affinity purified using the antigen to 0.4 mg/ml and supplied by the company.

Immunofluorescence assays

Chimeric GFP-expressing asexual lines were captured for live expression following incubation with 4′-6-diamidino-2-phenylindole (DAPI) at 0.2 μg/mL for 20 min and mounting under Menzel-Glaser 0.16 mm coverslips.

At 24 h post-blood feeding, *P. falciparum* NF54- and Δ*SOPT*-infected mosquitoes were dissected and bloodmeals pooled from 25 *An. stephensi* midguts. Contents were lysed with 0.15% saponin (w/v) in phosphate buffered saline (PBS), washed thrice and resuspended in 25 ml PBS. Resuspended pellets were placed at drops onto glass slides, air-dried and fixed with 4% paraformaldehyde (v/v) in PBS for 60 min at room temperature. Fixed cells were permeabilized with 0.5% Triton X-100 for 10 min and blocked overnight with 3% BSA (Sigma-Aldrich) in PBS. Cells were probed for 1 h at 37 ºC with mouse anti-Pfs25 (Barr *et al.*, 1991) (1:500) and rabbit anti-PfSOPT (10 μg/mL) antibodies in 3% BSA-PBS. After washing three times for 10 min each in PBS, samples were incubated for 30 min at 37 ºC with secondary AlexaFluor goat anti-mouse 488 and goat anti-rabbit 594 IgG antibodies (ThermoFisher) diluted 1:1000 in 3% BSA-PBS. Samples were again washed with PBS, stained with DAPI, air-dried, and mounted under cover glass with Fluormount-G (ThermoFisher). Images were acquired using a Deltavision Elite microscope (Applied Precision) using an Olympus 163×/1.42 PlanApoN objective equipped with a Coolsnap HQ2 charge-coupled device camera.

In vivo **cultivation of** ***P. berghei*** **for direct feeding assays**

Swiss Webster "donor" mice were infected via the intraperitoneal (i.p.) route with *P. berghei* ANKA *Pb*GFP-Luc$_{con}$ or *P. berghei* ANKA Δ*SOPT* GFP-luc (*Pb*Δ*SOPT/PIMMS2*). Parasitemia was monitored by Giemsa-stained tail blood smears. One week later, red blood cells from these infected donor mice were transferred to naïve mice via i.p. injection, which were used for direct feeding assays (DFAs) at three to four days post-inoculation. Mice with ≥1% parasitemia and exhibiting exflagellation

of microgametes by microscopy at 40x magnification, anesthetized with ketamine/xylazine via i.p. inoculation, and individually placed on top of a single container of 50 female *An. stephensi* (3-5 d old) mosquitoes. Mosquitoes were allowed to feed on mice for 15 min, after which any unfed mosquitoes were collected and discarded. Numbers of sexual stages (gametes/zygotes, retorts, ookinetes), oocysts, and sporozoites per mosquito were determined at 24 h, 10 d, and 21 d post-bloodfeeding, respectively, as described above.

Immunoblotting

Proteins were separated through 10% Bis-Tris polyacrylamide gels (Invitrogen), transferred to nitrocellulose and blocked in 10% skim milk/1x PBS/Tween (0.05%) and probed with mouse α-GFP (Roche; 1:500) and rabbit α-aldolase (1:4000) primary antibodies followed by horseradish peroxidase-conjugated secondary antibodies (Cell Signaling Technology) and detected by enhanced chemiluminescence (Amersham).

Assessment of *in vivo P. berghei* liver infection

C57BL/6 mice (female, 6-8 weeks) were injected with 10,000 *Pb*GFP-Luc$_{con}$ or *Pb*Δ*SOPT/PIMMS2* sporozoites obtained from freshly dissected salivary glands via intravenous (i.v.) tail vein injection. At 44 h post-infection, whole livers were dissected, and single cell suspensions generated with cell strainers. RNA was purified using TRI Reagent (Sigma) and cDNA prepared using a SensiFast cDNA synthesis kit (Bioline) according to manufacturers' instructions and RT-qPCR performed using a LightCycler 480 (Roche) to measure crossing points for the *P. berghei* 18S ribosomal RNA subunit and mouse hypoxanthine guanine phosphoribosyl transferase (Hprt) housekeeping gene using ΔC_T and oligonucleotides listed in Table S4. (Liehl *et al.*, 2014). Gene expression was calculated using the

$\Delta\Delta C_T$ method, with the mean of the control group as calibrator to which other samples were compared. To assess blood-stage infection, parasitemia was monitored daily by examination of Giemsa-stained thing blood smears. Animals were observed daily for signs of severe disease and those that developed hyperparasitemia (>15%), anemia, or neurological symptoms were CO_2 euthanized.

In vitro **cultivation and transmission of** ***P. berghei*** **ookinetes in standard membrane feeding assays**

One day following treatment with 1.2 mg phenylhydrazine-HCl (Sigma-Aldrich) in 200 µl in PBS via i.p. injection, Swiss Webster mice were inoculated with either *P. berghei Pb*GFP-Luc_{con} or Δ*SOPT/PIMMS2* parasites as described above. Upon detection of ≥1% parasitemia and exflagellation of microgametes by microscopy at 40x magnification three to four days later, mice were euthanized in a CO_2 chamber, and 0.8-1.0 mL blood was collected in a heparanized syringe via cardiac puncture. Blood was added directly to 10 mL ookinete medium (RPMI 1640 supplemented with 25 mM HEPES, 25 mM $NaHCO_3$, 100 mg/L neomycin, and 10% (v/v) fetal calf serum, pH 8.0) and incubated 20 h at 19ºC. Ookinetes were detected and quantified (ookinetes/mL) from Giemsa-stained blood smears, diluted to 800 ookinetes/µl and 50% haematocrit in uninfected mouse red blood cells and serum, and fed to *An. stephensi* mosquitoes in SMFAs as described above. Oocyst loads were determined at 10 d post-bloodfeeding.

Statistical analyses

All statistical analyses were performed using GraphPad Prism version 7.0 software. Student *t*-tests were used to compare numbers of round forms (gametes/zygotes), retorts, and ookinetes formed by wild type controls and Δ*SOPT* parasites. Mann-Whitney tests were used to evaluate differences in

median oocyst and sporozoite loads between wild type controls and Δ*SOPT* parasites. Multiple comparisons were performed by one-way ANOVA.

Ethics Statement

All experimental protocols involving mice were conducted in strict accordance with the recommendations in the National Statement on Ethical Conduct in Animal Research of the National Health and Medical Research Council and were reviewed and approved by the Walter and Eliza Hall Institute of Medical Research Animal Ethics Committee (AEC2014.030) and the Animal Experiments Committee of the Leiden University Medical Center (DEC 10099; DEC12042). The Dutch Experiments on Animal Act is established under European guidelines (EU directive no. 86/609/EEC regarding the Protection of Animals used for Experimental and Other Scientific Purposes). Experiments involving human erythrocytes and serum were approved by the Walter and Eliza Hall Institute of Medical Research Human Research Ethics Committee (HREC 86/17).

Acknowledgements

We thank Ryan Smith (Iowa State University) for helpful discussions regarding *SRPN6* expression and the Australian Red Cross Melbourne for human erythrocytes and serum. Monoclonal Antibody 4B7 anti-*Plasmodium falciparum* 25 kDa Gamete Surface Protein (Pfs25), MRA-28, was obtained through BEI Resources NIAID, NIH, contributed by David C. Kaslow. This work was supported by the Australian National Health and Medical Research Council (Project Grant 1049811), Human Frontiers Science Program (RGY0073/2012), and a Victorian State Government Operational Infrastructure Support and Australian Government NHMRC IRIISS. JAB was a Queen Elizabeth II Fellow of the

Australian Research Council (DP110105395). The funders had no role in study design, data collection, and interpretation, or the decision to submit the work for publication.

Author Contributions

JSA, CJ, MTO, SL, PL, KKH, PR, SME, CJT, TA and JAB performed and analyzed experiments, SMK, MMM and JAB designed and interpreted experiments, JSA and JAB conceived the study, all authors contributed to writing the manuscript.

Competing financial interests

The authors declare no competing financial interests.

References

Abraham, E.G., Pinto, S.B., Ghosh, A., Vanlandingham, D.L., Budd, A., Higgs, S., Kafatos, F.C., Jacobs-Lorena, M., and Michel, K. (2005) An immune-responsive serpin, SRPN6, mediates mosquito defense against malaria parasites. *Proc Natl Acad Sci U S A* **102**: 16327-16332.

Alam, A., Bhatnagar, R.K., and Chauhan, V.S. (2012) Expression and characterization of catalytic domain of Plasmodium falciparum subtilisin-like protease 3. *Mol Biochem Parasitol* **183**: 84-89.

Angrisano, F., Riglar, D.T., Sturm, A., Volz, J.C., Delves, M.J., Zuccala, E.S., Turnbull, L., Dekiwadia, C., Olshina, M.A., Marapana, D.S., Wong, W., Mollard, V., Bradin, C.H., Tonkin, C.J., Gunning, P.W., Ralph, S.A., Whitchurch, C.B., Sinden, R.E., Cowman, A.F., McFadden, G.I., and Baum, J. (2012) Spatial localisation of actin filaments across developmental stages of the malaria parasite. *PLoS One* **7**: e32188.

Arastu-Kapur, S., Ponder, E.L., Fonovic, U.P., Yeoh, S., Yuan, F., Fonovic, M., Grainger, M., Phillips, C.I., Powers, J.C., and Bogyo, M. (2008) Identification of proteases that regulate erythrocyte rupture by the malaria parasite Plasmodium falciparum. *Nat Chem Biol* **4**: 203-213.

Barale, J.C., Blisnick, T., Fujioka, H., Alzari, P.M., Aikawa, M., Braun-Breton, C., and Langsley, G. (1999) *Plasmodium falciparum* subtilisin-like protease 2, a merozoite candidate for the merozoite surface protein 1-42 maturase. *Proc. Natl. Acad. Sci. U S A* **96**: 6445-6450.

Barr, P.J., Green, K.M., Gibson, H.L., Bathurst, I.C., Quakyi, I.A., and Kaslow, D.C. (1991) Recombinant Pfs25 protein of Plasmodium falciparum elicits malaria transmission-blocking immunity in experimental animals. *J. Exp. Med.* **174**: 1203-1208.

Bendtsen, J.D., Nielsen, H., von Heijne, G., and Brunak, S. (2004) Improved prediction of signal peptides: SignalP 3.0. *J. Mol. Biol.* **340**: 783-795.

Bunnik, E.M., Chung, D.W., Hamilton, M., Ponts, N., Saraf, A., Prudhomme, J., Florens, L., and Le Roch, K.G. (2013) Polysome profiling reveals translational control of gene expression in the human malaria parasite Plasmodium falciparum. *Genome biology* **14**: R128.

Bushell, E., Gomes, A.R., Sanderson, T., Anar, B., Girling, G., Herd, C., Metcalf, T., Modrzynska, K., Schwach, F., Martin, R.E., Mather, M.W., McFadden, G.I., Parts, L., Rutledge, G.G., Vaidya, A.B., Wengelnik, K., Rayner, J.C., and Billker, O. (2017) Functional Profiling of a Plasmodium Genome Reveals an Abundance of Essential Genes. *Cell* **170**: 260-272 e268.

Chen, L., Xu, Y., Wong, W., Thompson, J.K., Healer, J., Goddard-Borger, E.D., Lawrence, M.C., and Cowman, A.F. (2017) Structural basis for inhibition of erythrocyte invasion by antibodies to Plasmodium falciparum protein CyRPA. *eLife* **6**.

Child, M.A., Epp, C., Bujard, H., and Blackman, M.J. (2010) Regulated maturation of malaria merozoite surface protein-1 is essential for parasite growth. *Mol Microbiol* **78**: 187-202.

Collins, C.R., Hackett, F., Atid, J., Tan, M.S.Y., and Blackman, M.J. (2017) The Plasmodium falciparum pseudoprotease SERA5 regulates the kinetics and efficiency of malaria parasite egress from host erythrocytes. *PLoS Pathog* **13**: e1006453.

Danielli, A., Barillas-Mury, C., Kumar, S., Kafatos, F.C., and Loukeris, T.G. (2005) Overexpression and altered nucleocytoplasmic distribution of Anopheles ovalbumin-like SRPN10 serpins in Plasmodium-infected midgut cells. *Cell Microbiol* **7**: 181-190.

Dessens, J.T., Beetsma, A.L., Dimopoulos, G., Wengelnik, K., Crisanti, A., Kafatos, F.C., and R.E., S. (1999) CTRP is essential for mosquito infection by malaria ookinetes. *EMBO J.* **18**: 6221-6227.

Dessens, J.T., Siden-Kiamos, I., Mendoza, J., Mahairaki, V., Khater, E., Vlachou, D., Xu, X.J., Kafatos, F.C., Louis, C., Dimopoulos, G., and Sinden, R.E. (2003) SOAP, a novel malaria ookinete protein involved in mosquito midgut invasion and oocyst development. *Mol Microbiol* **49**: 319-329.

Dutta, S., Haynes, J.D., Barbosa, A., Ware, L.A., Snavely, J.D., Moch, J.K., Thomas, A.W., and Lanar, D.E. (2005) Mode of action of invasion-inhibitory antibodies directed against apical membrane antigen 1 of Plasmodium falciparum. *Infect Immun* **73**: 2116-2122.

Eappen, A.G., Smith, R.C., and Jacobs-Lorena, M. (2013) Enterobacter-activated mosquito immune responses to Plasmodium involve activation of SRPN6 in Anopheles stephensi. *PLoS One* **8**: e62937.

Ecker, A., Bushell, E.S., Tewari, R., and Sinden, R.E. (2008) Reverse genetics screen identifies six proteins important for malaria development in the mosquito. *Mol Microbiol* **70**: 209-220.

El Bakkouri, M., Rathore, S., Calmettes, C., Wernimont, A.K., Liu, K., Sinha, D., Asad, M., Jung, P., Hui, R., Mohmmed, A., and Houry, W.A. (2013) Structural insights into the inactive subunit of the apicoplast-localized caseinolytic protease complex of Plasmodium falciparum. *J Biol Chem* **288**: 1022-1031.

Eyers, P.A., and Murphy, J.M. (2016) The evolving world of pseudoenzymes: proteins, prejudice and zombies. *BMC Biol* **14**: 98.

Favuzza, P., Guffart, E., Tamborrini, M., Scherer, B., Dreyer, A.M., Rufer, A.C., Erny, J., Hoernschemeyer, J., Thoma, R., Schmid, G., Gsell, B., Lamelas, A., Benz, J., Joseph, C., Matile, H., Pluschke, G., and Rudolph, M.G. (2017) Structure of the malaria vaccine candidate antigen CyRPA and its complex with a parasite invasion inhibitory antibody. *eLife* **6**.

Fleck, S.L., Birdsall, B., Babon, J., Dluzewski, A.R., Martin, S.R., Morgan, W.D., Angov, E., Kettleborough, C.A., Feeney, J., Blackman, M.J., and Holder, A.A. (2003) Suramin and suramin analogues inhibit merozoite surface protein-1 secondary processing and erythrocyte invasion by the malaria parasite Plasmodium falciparum. *J Biol Chem* **278**: 47670-47677.

Florens, L., Washburn, M.P., Raine, J.D., Anthony, R.M., Grainger, M., Haynes, J.D., Moch, J.K., Muster, N., Sacci, J.B., Tabb, D.L., Witney, A.A., Wolters, D., Wu, Y., Gardner, M.J., Holder, A.A., Sinden, R.E., Yates, J.R., and Carucci, D.J. (2002) A proteomic view of the *Plasmodium falciparum* life cycle. *Nature* **419**: 520-526.

Gattiker, A., Gasteiger, E., and Bairoch, A. (2002) ScanProsite: a reference implementation of a PROSITE scanning tool. *Appl Bioinformatics* **1**: 107-108.

Gething, P.W., Casey, D.C., Weiss, D.J., Bisanzio, D., Bhatt, S., Cameron, E., Battle, K.E., Dalrymple, U., Rozier, J., Rao, P.C., Kutz, M.J., Barber, R.M., Huynh, C., Shackelford, K.A., Coates, M.M., Nguyen, G., Fraser, M.S., Kulikoff, R., Wang, H., Naghavi, M., Smith, D.L., Murray, C.J., Hay, S.I., and Lim, S.S. (2016) Mapping *Plasmodium falciparum* Mortality in Africa between 1990 and 2015. *N Engl J Med* **375**: 2435-2445.

Ghosh, A.K., Coppens, I., Gardsvoll, H., Ploug, M., and Jacobs-Lorena, M. (2011) Plasmodium ookinetes coopt mammalian plasminogen to invade the mosquito midgut. *Proc Natl Acad Sci U S A* **108**: 17153-17158.

Green, J.L., Hinds, L., Grainger, M., Knuepfer, E., and Holder, A.A. (2006) Plasmodium thrombospondin related apical merozoite protein (PTRAMP) is shed from the surface of merozoites by PfSUB2 upon invasion of erythrocytes. *Mol Biochem Parasitol* **150**: 114-117.

Han, Y.S., Thompson, J., Kafatos, F.C., and Barillas-Mury, C. (2000) Molecular interactions between Anopheles stephensi midgut cells and Plasmodium berghei: the time bomb theory of ookinete invasion of mosquitoes. *EMBO J* **19**: 6030-6040.

Harris, P.K., Yeoh, S., Dluzewski, A.R., O'Donnell R, A., Withers-Martinez, C., Hackett, F., Bannister, L.H., Mitchell, G.H., and Blackman, M.J. (2005a) Molecular identification of a malaria merozoite surface sheddase. *PLoS Pathog.* **1**: e29.

Harris, P.K., Yeoh, S., Dluzewski, A.R., O'Donnell, R.A., Withers-Martinez, C., Hackett, F., Bannister, L.H., Mitchell, G.H., and Blackman, M.J. (2005b) Molecular identification of a malaria merozoite surface sheddase. *PLoS Pathog* **1**: 241-251.

Hiller, N.L., Bhattacharjee, S., van Ooij, C., Liolios, K., Harrison, T., Lopez-Estrano, C., and Haldar, K. (2004) A host-targeting signal in virulence proteins reveals a secretome in malarial infection. *Science* **306**: 1934-1937.

Howell, S.A., Hackett, F., Jongco, A.M., Withers-Martinez, C., Kim, K., Carruthers, V.B., and Blackman, M.J. (2005) Distinct mechanisms govern proteolytic shedding of a key invasion protein in apicomplexan pathogens. *Mol. Microbiol.* **57**: 1342-1356.

Janse, C.J., Franke-Fayard, B., Mair, G.R., Ramesar, J., Thiel, C., Engelmann, S., Matuschewski, K., van Gemert, G.J., Sauerwein, R.W., and Waters, A.P. (2006a) High efficiency transfection of Plasmodium berghei facilitates novel selection procedures. *Mol. Biochem. Parasitol.* **145**: 60-70.

Janse, C.J., Ramesar, J., and Waters, A.P. (2006b) High-efficiency transfection and drug selection of genetically transformed blood stages of the rodent malaria parasite Plasmodium berghei. *Nature protocols* **1**: 346-356.

Kadota, K., Ishino, T., Matsuyama, T., Chinzei, Y., and Yuda, M. (2004) Essential role of membrane-attack protein in malarial transmission to mosquito host. *Proc Natl Acad Sci U S A* **101**: 16310-16315.

Kariu, T., Ishino, T., Yano, K., Chinzei, Y., and Yuda, M. (2006) CelTOS, a novel malarial protein that mediates transmission to mosquito and vertebrate hosts. *Mol Microbiol* **59**: 1369-1379.

Kelley, L.A., Mezulis, S., Yates, C.M., Wass, M.N., and Sternberg, M.J. (2015) The Phyre2 web portal for protein modeling, prediction and analysis. *Nature protocols* **10**: 845-858.

Knuepfer, E., Rug, M., and Cowman, A.F. (2005) Function of the plasmodium export element can be blocked by green fluorescent protein. *Mol Biochem Parasitol* **142**: 258-262.

Liehl, P., Zuzarte-Luis, V., Chan, J., Zillinger, T., Baptista, F., Carapau, D., Konert, M., Hanson, K.K., Carret, C., Lassnig, C., Muller, M., Kalinke, U., Saeed, M., Chora, A.F., Golenbock, D.T., Strobl, B., Prudencio, M., Coelho, L.P., Kappe, S.H., Superti-Furga, G., Pichlmair, A., Vigario, A.M., Rice, C.M., Fitzgerald, K.A., Barchet, W., and Mota, M.M. (2014) Host-cell sensors for Plasmodium activate innate immunity against liver-stage infection. *Nat Med* **20**: 47-53.

Lin, J.W., Annoura, T., Sajid, M., Chevalley-Maurel, S., Ramesar, J., Klop, O., Franke-Fayard, B.M., Janse, C.J., and Khan, S.M. (2011) A novel 'gene insertion/marker out' (GIMO) method for transgene expression and gene complementation in rodent malaria parasites. *PLoS One* **6**: e29289.

Lopaticki, S., Yang, A.S.P., John, A., Scott, N.E., Lingford, J.P., O'Neill, M.T., Erickson, S.M., McKenzie, N.C., Jennison, C., Whitehead, L.W., Douglas, D.N., Kneteman, N.M., Goddard-Borger, E.D., and Boddey, J.A. (2017) Protein O-fucosylation in Plasmodium falciparum ensures efficient infection of mosquito and vertebrate hosts. *Nat Commun* **8**: 561.

Lopez-Barragan, M.J., Lemieux, J., Quinones, M., Williamson, K.C., Molina-Cruz, A., Cui, K., Barillas-Mury, C., Zhao, K., and Su, X.Z. (2011) Directional gene expression and antisense transcripts in sexual and asexual stages of *Plasmodium falciparum*. *BMC Genomics* **12**: 587.

Marti, M., Good, R.T., Rug, M., Knuepfer, E., and Cowman, A.F. (2004) Targeting malaria virulence and remodeling proteins to the host erythrocyte. *Science* **306**: 1930-1933.

Pinto, S.B., Kafatos, F.C., and Michel, K. (2008) The parasite invasion marker SRPN6 reduces sporozoite numbers in salivary glands of Anopheles gambiae. *Cell Microbiol* **10**: 891-898.

Reynolds, S.L., and Fischer, K. (2015) Pseudoproteases: mechanisms and function. *Biochem J* **468**: 17-24.

Ruecker, A., Shea, M., Hackett, F., Suarez, C., Hirst, E.M., Milutinovic, K., Withers-Martinez, C., and Blackman, M.J. (2012) Proteolytic activation of the essential parasitophorous vacuole cysteine protease SERA6 accompanies malaria parasite egress from its host erythrocyte. *J Biol Chem* **287**: 37949-37963.

Saliba, K.S., and Jacobs-Lorena, M. (2013) Production of *Plasmodium falciparum* gametocytes in vitro. *Methods Mol Biol* **923**: 17-25.

Santos, J.M., Egarter, S., Zuzarte-Luis, V., Kumar, H., Moreau, C.A., Kehrer, J., Pinto, A., Costa, M.D., Franke-Fayard, B., Janse, C.J., Frischknecht, F., and Mair, G.R. (2017) Malaria parasite LIMP protein regulates sporozoite gliding motility and infectivity in mosquito and mammalian hosts. *eLife* **6**.

Sargeant, T.J., Marti, M., Caler, E., Carlton, J.M., Simpson, K., Speed, T.P., and Cowman, A.F. (2006) Lineage-specific expansion of proteins exported to erythrocytes in malaria parasites. *Genome Biol.* **7**: R12.

Sievers, F., Wilm, A., Dineen, D., Gibson, T.J., Karplus, K., Li, W., Lopez, R., McWilliam, H., Remmert, M., Soding, J., Thompson, J.D., and Higgins, D.G. (2011) Fast, scalable generation of high-quality protein multiple sequence alignments using Clustal Omega. *Mol Syst Biol* **7**: 539.

Siezen, R.J., and Leunissen, J.A. (1997) Subtilases: the superfamily of subtilisin-like serine proteases. *Protein Sci* **6**: 501-523.

Silmon de Monerri, N.C., Flynn, H.R., Campos, M.G., Hackett, F., Koussis, K., Withers-Martinez, C., Skehel, J.M., and Blackman, M.J. (2011) Global identification of multiple substrates for Plasmodium falciparum SUB1, an essential malarial processing protease. *Infect Immun* **79**: 1086-1097.

Sinden, R.E. (2010) A biologist's perspective on malaria vaccine development. *Hum Vaccin* **6**: 3-11.

Sleebs, B.E., Lopaticki, S., Marapana, D.S., O'Neill, M.T., Rajasekaran, P., Gazdik, M., Gunther, S., Whitehead, L.W., Lowes, K.N., Barfod, L., Hviid, L., Shaw, P.J., Hodder, A.N., Smith, B.J., Cowman, A.F., and Boddey, J.A. (2014) Inhibition of Plasmepsin V activity demonstrates its essential role in protein export, PfEMP1 display, and survival of malaria parasites. *PLoS Biol* **12**: e1001897.

Smith, R.C., Eappen, A.G., Radtke, A.J., and Jacobs-Lorena, M. (2012) Regulation of anti-*Plasmodium* immunity by a LITAF-like transcription factor in the malaria vector *Anopheles gambiae*. *PLoS Pathog* **8**: e1002965.

Stallmach, R., Kavishwar, M., Withers-Martinez, C., Hackett, F., Collins, C.R., Howell, S.A., Yeoh, S., Knuepfer, E., Atid, A.J., Holder, A.A., and Blackman, M.J. (2015) Plasmodium falciparum SERA5 plays a non-enzymatic role in the malarial asexual blood-stage lifecycle. *Mol Microbiol* **96**: 368-387.

Steel, R.W.J., Pei, Y., Camargo, N., Kaushansky, A., Dankwa, D.A., Martinson, T., Nguyen, T., Betz, W., Cardamone, H., Vigdorovich, V., Dambrauskas, N., Carbonetti, S., Vaughan, A.M., Sather, D.N., and Kappe, S.H.I. (2018) Plasmodium yoelii S4/CelTOS is important for sporozoite gliding motility and cell traversal. *Cell Microbiol* **20**.

Suarez, C., Volkmann, K., Gomes, A.R., Billker, O., and Blackman, M.J. (2013) The malarial serine protease SUB1 plays an essential role in parasite liver stage development. *PLoS Pathog* **9**: e1003811.

Suarez-Cortes, P., Sharma, V., Bertuccini, L., Costa, G., Bannerman, N.L., Sannella, A.R., Williamson, K., Klemba, M., Levashina, E.A., Lasonder, E., and Alano, P. (2016) Comparative Proteomics and Functional Analysis Reveal a Role of Plasmodium falciparum Osmiophilic Bodies in Malaria Parasite Transmission. *Mol Cell Proteomics* **15**: 3243-3255.

Tawk, L., Lacroix, C., Gueirard, P., Kent, R., Gorgette, O., Thiberge, S., Mercereau-Puijalon, O., Menard, R., and Barale, J.C. (2013) A key role for Plasmodium subtilisin-like SUB1 protease in egress of malaria parasites from host hepatocytes. *J Biol Chem* **288**: 33336-33346.

Templeton, T.J., Kaslow, D.C., and Fidock, D.A. (2000) Developmental arrest of the human malaria parasite *Plasmodium falciparum* within the mosquito midgut via *CTRP* gene disruption. *Mol. Microbiol.* **36**: 1-9.

Tomas, A.M., Margos, G., Dimopoulos, G., van Lin, L.H., de Koning-Ward, T.F., Sinha, R., Lupetti, P., Beetsma, A.L., Rodriguez, M.C., Karras, M., Hager, A., Mendoza, J., Butcher, G.A., Kafatos, F., Janse, C.J., Waters, A.P., and Sinden, R.E. (2001) P25 and P28 proteins of the malaria ookinete surface have multiple and partially redundant functions. *EMBO J* **20**: 3975-3983.

Trottein, F., Triglia, T., and Cowman, A.F. (1995) Molecular cloning of a gene from *Plasmodium falciparum* that codes for a protein sharing motifs found in adhesive molecules from mammals and plasmodia. *Mol. Biochem. Parasitol.* **74**: 129-141.

Ukegbu, C.V., Akinosoglou, K.A., Christophides, G.K., and Vlachou, D. (2017) Plasmodium berghei PIMMS2 promotes ookinete invasion of the Anopheles gambiae mosquito midgut. *Infect Immun*.

Uzureau, P., Barale, J.C., Janse, C.J., Waters, A.P., and Breton, C.B. (2004) Gene targeting demonstrates that the Plasmodium berghei subtilisin PbSUB2 is essential for red cell invasion and reveals spontaneous genetic recombination events. *Cell Microbiol* **6**: 65-78.

Waller, R.F., Reed, M.B., Cowman, A.F., and McFadden, G.I. (2000) Protein trafficking to the plastid of *Plasmodium falciparum* is via the secretory pathway. *EMBO J.* **19**: 1794-1802.

Withers-Martinez, C., Strath, M., Hackett, F., Haire, L.F., Howell, S.A., Walker, P.A., Christodoulou, E., Dodson, G.G., and Blackman, M.J. (2014) The malaria parasite egress protease SUB1 is a calcium-dependent redox switch subtilisin. *Nature communications* **5**: 3726.

Yuda, M., Sakaida, H., and Chinzel, Y. (1999) Targeted Disruption of the *Plasmodium berghei* CTRP Gene Reveals Its Essential Role in Malaria Infection of the Vector Mosquito. *J. Exp. Med.* **190**: 1711-1715.

Yuda, M., Yano, K., Tsuboi, T., Torii, M., and Chinzei, Y. (2001) von Willebrand Factor A domain-related protein, a novel microneme protein of the malaria ookinete highly conserved throughout Plasmodium parasites. *Mol Biochem Parasitol* **116**: 65-72.

Figure Legends

Fig. 1. SOPT is a conserved subtilisin-like protein in *Plasmodium*.

A. Homology model of *P. falciparum* SOPT (T166-K552, light blue) overlaid on the X-ray crystal structure of *P. falciparum* SUB1 (T366-K669, pale green, 4LVN, RMS = 2.25 Å) (Withers-Martinez *et al.*, 2014). The red catalytic residues (D372, H428, S606) are from PfSUB1.

B. Sequence alignment of SOPT from *P. falciparum* (T166-K552) and with *P. falciparum* SUB1 (T366-K669), showing predicted secondary structures and catalytic residues (red).

C. A multiple sequence alignment of full-length SOPT from ten *Plasmodium* species was used to identify residues in the catalytic triad (red). Pf, *P. falciparum* 3D7; Pr, *P. reichenowi* CDC; Pm, *P. malariae* UG01; Py, *P. yoelii* 17X; Pc, *P. chabaudi chabaudi*; Pb, *P. berghei* ANKA; Pg, *P. gallinaceum* 8A; Po, *P. ovale curtisi* GH01; Pv, *P. vivax* Sal-1; Pk, *P. knowlesi* strain H.

D. A multiple sequence alignment of the N-terminus of SOPT from six *Plasmodium* species shows conservation of a PEXEL-like sequence, RxLxE, located C-terminal of the signal peptide (red line). Pf, *P. falciparum* 3D7; Pr, *P. reichenowi* CDC; Pv, *P. vivax* Sal-1; Pcy, *P. cynomolgi* Strain B; Pk, *P. knowlesi* strain H; Pb, *P. berghei* ANKA.

E. Structure and amino acid sequence of the PfSOPT_1-62–GFP chimera. Twenty residues were included A spacer (20 aa) was included between the PEXEL-like sequence RILEE and GFP. The protein was expressed from the *CRT* gene promoter.

F. Immunoblot of infected erythrocytes with anti-GFP antibodies shows expression of PfSOPT_1-62-GFP (arrow). 'GFP only' represents degradation to a GFP remnant in the food vacuole that is commonly observed in *P. falciparum*.

G. Immunofluorescence microscopy images showing PfSOPT_1-62-GFP is secreted to the parasitophorous vacuole in infected erythrocytes but is not exported. Scale bar, 5 μM.

Fig. 2. Genetic disruption and characterization of SOPT in *P. falciparum*.

A. Schematic representation of allelic exchange to genetically disrupt the *SOPT* gene in *P. falciparum* NF54. *CDUP* refers to *cytosine deaminase/uracil phosphoribosyl transferase* gene used for negative selection with 5'-fluorocytosine (5-FC).

B. Southern blot analysis of NF54 and Δ*SOPT* clones D4 and E8. Genomic DNA was digested with HincII/BamHI and hybridized with 5' and 3' probes respectively.

C. Asexual growth rate of NF54 and Δ*SOPT* parasites after one-cycle (approx. 48 hours). No significant differences (n.s.) were found between NF54 and either mutant clone, as determined by one-way Kuskal-Wallis ANOVA (p=0.3131).

D. Percentage of stage V gametocytes produced by NF54 and Δ*SOPT* parasites 17 days after initiation of gametocytogenesis. No significant differences (n.s.) were found between NF54 and either mutant clone, as determined by one-way Kuskal-Wallis ANOVA (p=0.8071). Data in (C) and (D) represent mean ± SEM from two and three independent experiments, respectively.

E. Immunofluorescence microscopy of *P. falciparum* ookinetes after dissection from mosquito midguts. Top: SOPT is expressed in NF54 ookinetes (red) and partly co-localizes with the surface protein Pfs25 (green). Bottom: No expression of SOPT is detected in Δ*SOPT* ookinetes but Pfs25 expression is detected.

Fig. 3. SOPT facilitates *P. falciparum* ookinete infection of *Anopheles stephensi* midguts.

A. *P. falciparum* Δ*SOPT* parasites form comparable numbers of round forms (gametes/zygotes), retorts, and ookinetes as NF54 controls following infection of *Anopheles stephensi* mosquitoes in standard membrane feeding assays (SMFAs). Data represent mean ± SEM from three independent biological replicates (n=25 mosquitoes/replicate). No significant differences (n.s.) were found between NF54 and either mutant clone, as determined by one-way Kruskal-Wallis ANOVA (p=0.4985).

B. *P. falciparum* Δ*SOPT* parasites produce fewer oocysts per mosquito midgut than NF54 controls. Data represent three independent biological replicates. Red horizontal lines indicate median oocyst load. *** $p<0.0001$, determined by the Mann-Whitney test.

C. *P. falciparum* Δ*SOPT* parasites generate fewer salivary gland sporozoites per mosquito than NF54 controls. Data represent three independent biological replicates. Red horizontal lines indicate median sporozoite load. *** $p<0.0001$, determined by the Mann-Whitney test.

D and E. RT-qPCR quantification of *An. stephensi SRPN6* mRNA expression relative to either the housekeeping gene *An. stephensi rps7* (D) or *P. falciparum* ookinete gene *CTRP* (E) in midguts from mosquitoes that were sugarfed (uninfected) or fed infected blood containing NF54 or Δ*SOPT* D4 or E8 clones. Data are from n=25 midguts per condition per experiment from 4 independent experiments, pooled and analyzed by a one-way ANOVA. *** $p<0.0001$ and ** $p<0.001$ compared to NF54 using a Dunnet's post-hoc test.

Fig. 4. SOPT function is conserved in different *Plasmodium* species.

A. Schematic representation of allelic exchange to genetically disrupt the *PbSOPT* gene (also called *PIMMS2*).

B. PCR analysis of PbGFP-Luc$_{con}$ and Pb**Δ***SOPT/PIMMS2* 1482 cl1. Sizes of amplicons are indicated in (A).

C. Pb**Δ***SOPT/PIMMS2* parasites form comparable numbers of round forms (gametes/zygotes), retorts, and ookinetes as parental controls (PbGFP-Luc$_{con}$) in *An. stephensi* mosquitoes following direct feeding assays (DFAs) with BALB/c mice. Data represent mean ± SEM from three independent biological replicates (n=25 mosquitoes/replicate). * $p<0.05$ determined by t-test.

D. Pb**Δ***SOPT/PIMMS2* parasites produce fewer oocysts per mosquito than PbGFP-Luc$_{con}$ following infection of *An. stephensi* mosquitoes in DFAs with BALB/c mice. Red horizontal lines indicate median oocyst load. *** $p<0.0001$ determined by the Mann-Whitney test.

E. Pb**Δ***SOPT/PIMMS2* parasites produce fewer sporozoites per mosquito than PbGFP-Luc$_{con}$ following infection of *An. stephensi* mosquitoes in DFAs with BALB/c mice. Data in (D) and (E) are from three independent experiments, each comprised of n=3 *Pb*GFP-Luc$_{con}$ and n=3 PbΔ*SOPT/PIMMS2*-infected mice. Red horizontal lines indicate median sporozoite load. *** $p<0.0001$ determined by the Mann-Whitney test.

Fig. 5. PbSOPT/PIMMS2 is dispensable for ookinete development, sporozoite infectivity and establishing patent blood infections.

A. Pb**Δ***SOPT/PIMMS2* parasites produce equal numbers of ookinetes in *in vitro* cultures compared to PbGFP-Luc$_{con}$ controls. Data are mean ± SEM from 4 independent experiments. No significant differences (n.s.) were observed using the Mann Whitney test ($p=0.6742$).

B. *In vitro* cultured ookinetes form fewer oocysts per mosquito when equivalent numbers are fed to *An. stephensi* mosquitoes in SMFAs. Data shown are pooled from four independent experiments. Red horizontal lines indicate median oocyst load. *** $p<0.0001$ using the Mann Whitney test.

C. Liver load of Pb*ΔSOPT/PIMMS2* and *Pb*GFP-Luc$_{con}$ parasites, measured by RT-qPCR 44 h post-i.v. injection with 10,000 sporozoites per mouse. Data are mean ± SEM from 2 independent experiments each with groups of 5 mice. *P. berghei* 18S rRNA expression in *PbΔSOPT/PIMMS2* parasites was normalized to that of *Pb*GFP-Luc$_{con}$ controls. Mouse *HPRT* was used as a housekeeping gene.

D. Mean parasitemia ±SEM of C57BL/6 mice that developed patent blood-stage infections following i.v. injection with 10,000 sporozoites from either *Pb*GFP-Luc$_{con}$ (n=5/5) or *ΔSOPT/PIMMS2* (n=4/6) infected mosquitoes.

Fig. S1. Detailed generation and genotyping of Pb*ΔSOPT/PIMMS2* parasites.

A. Schematic showing the generation of Pb*ΔSOPT/PIMMS2* (ΔPBANKA_1106900 (1482cl1). The DNA-construct pL1500 is designed to disrupt the target gene by double cross-over homologous recombination. The construct was generated by an adapted 'Anchor-tagging' PCR-based method employing a 2-step PCR reaction. In the first PCR step two-flanking fragments of PBANKA_1106900 were amplified from genomic DNA with the primers 4744/4745 (5′) and 4746/4747 (3′). Both primers, 4745 and 4747, have 5′-terminal extensions homologues to the *hdhfr* selectable marker cassette (SM) obtained from plasmid pL0040 (digested with restriction enzymes *Xho*I and *Not*I). Primers 4744 and 4747 have 5′-terminal overhang with an anchor-tag suitable for the second PCR step. These fragments were then annealed to either side of the SM with anchor-tag primers 4661/4662, resulting in the second PCR fragment. To remove the 'anchor', the final PCR fragment was digested with *Asp*718 and *Sca*I (primers 4744 and 4747 contained *Asp*718 and *Sca*I restriction enzyme sites, respectively), resulting in construct pL1500. See Supplementary Table 4 for the sequence of the primers.

B. Confirmation of correct integration of the gene-deletion construct pL1500 in mutant 1482cl1 by Southern analysis of PFG-separated chromosomes (left panel) and by diagnostic PCR (right panel).

Hybridization of separated chromosomes (chr.) with the 3′-UTR *dhfr/ts* probe recognizes the integrated construct on chr. 11, the endogenous *dhfr/ts* gene on chr. 7 and the reporter GFP-Luc_{con} construct in chr. 3 of the parent reference *P. berghei* ANKA PbGFP-Luc_{con}. Diagnostic PCR confirms the correct disruption of PBANKA_1106900. M: selectable marker (primers L307C/3187); 5′-integration (primers 4286/4770); 3′-integration event (primers 4471/4287); O (open reading frame; primers 4435/4436).

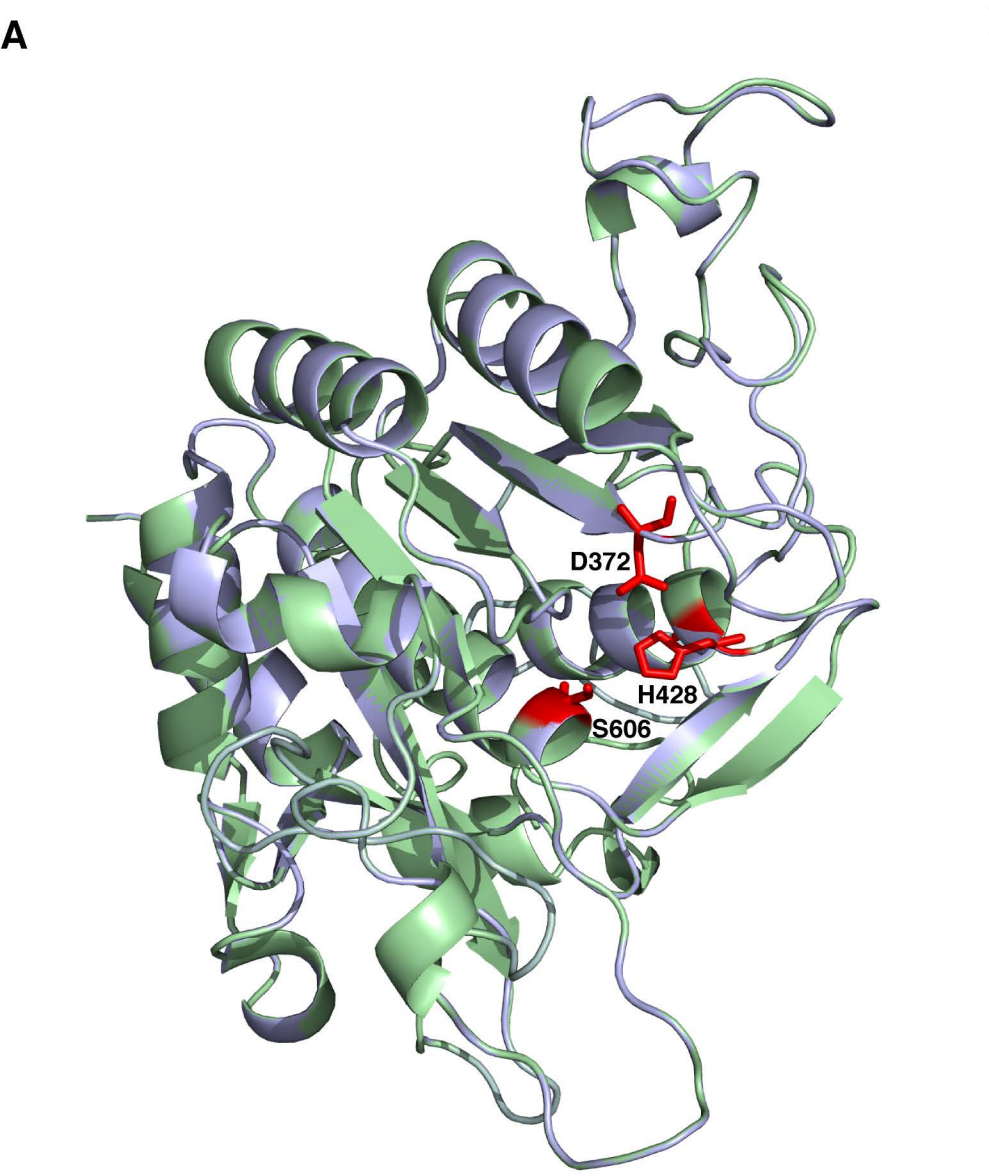
A
D372
H428
S606

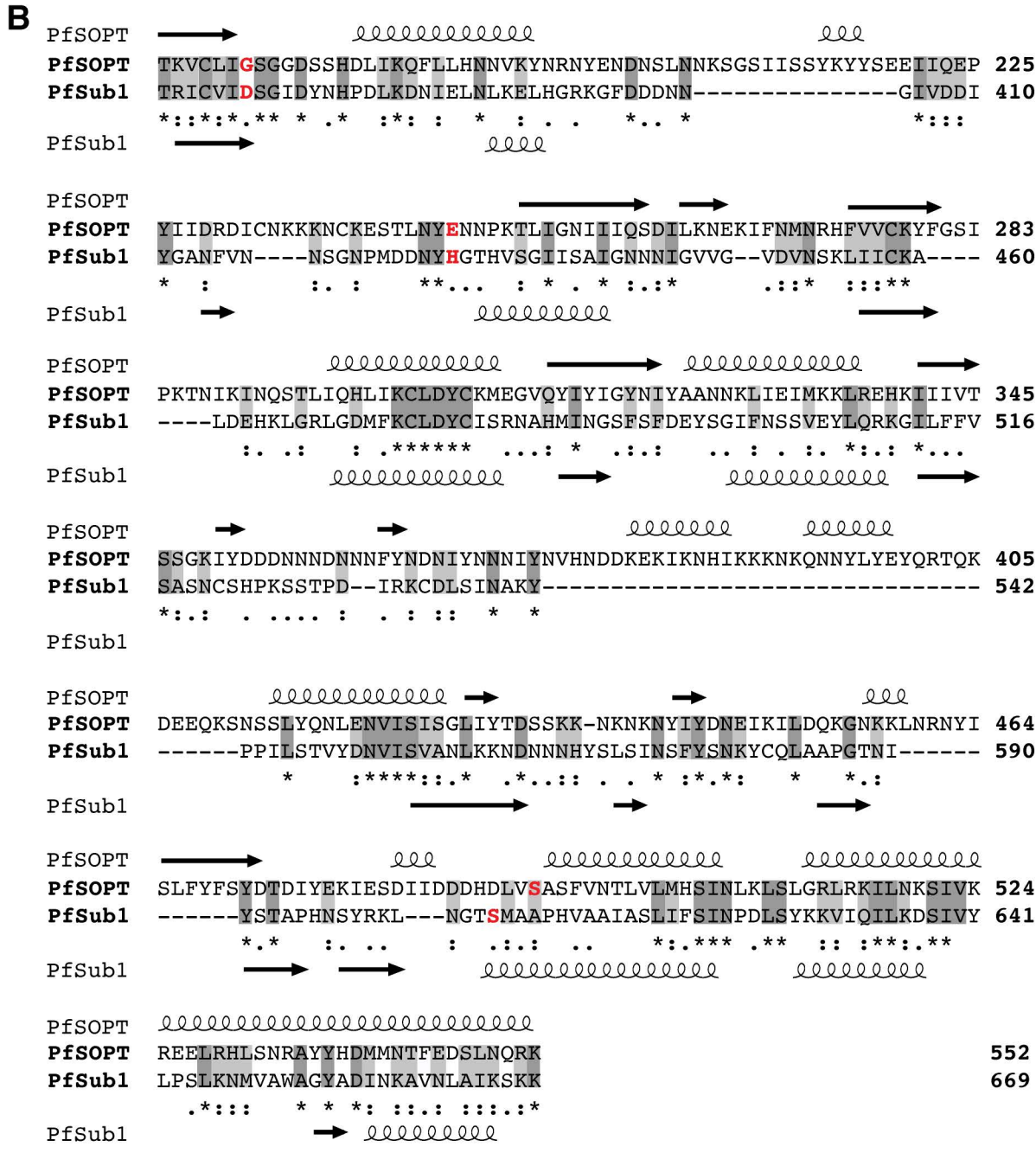
B
PfSOPT
PfSOPT TKVCLIGSGGDSSHDLIKQFLLHNNVKYNRNYENDNSLNNKSGSIISSYKYYSEEIIQEP 225
PfSub1 TRICVIDSGIDYNHPDLKDNIELNLKELHGRKGFDDDNN---------------GIVDDI 410
PfSub1
PfSOPT
PfSOPT YIIDRDICNKKKNCKESTLNYENNPKTLIGNIIIQSDILKNEKIFNMNRHFVVCKYFGSI 283
PfSub1 YGANFVN----NSGNPMDDNYHGTHVSGIISAIGNNNIGVVG--VDVNSKLIICKA---- 460
PfSub1
PfSOPT
PfSOPT PKTNIKINQSTLIQHLIKCLDYCKMEGVQYIYIGYNIYAANNKLIEIMKKLREHKIIIVT 345
PfSub1 ----LDEHKLGRLGDMFKCLDYCISRNAHMINGSFSFDEYSGIFNSSVEYLQRKGILFFV 516
PfSub1
PfSOPT
PfSOPT SSGKIYDDDNNNDNNNFYNDNIYNNNIYNVHNDDKEKIKNHIKKKNKQNNYLYEYQRTQK 405
PfSub1 SASNCSHPKSSTPD--IRKCDLSINAKY------------------------------ 542
PfSub1
PfSOPT
PfSOPT DEEQKSNSSLYQNLENVISISGLIYTDSSKK-NKNKNYIYDNEIKILDQKGNKKLNRNYI 464
PfSub1 ------PPILSTVYDNVISVANLKKNDNNNHYSLSINSFYSNKYCQLAAPGTNI------ 590
PfSub1
PfSOPT
PfSOPT SLFYFSYDTDIYEKIESDIIDDDHDLVSASFVNTLVLMHSINLKLSLGRLRKILNKSIVK 524
PfSub1 ------YSTAPHNSYRKL---NGTSMAAPHVAAIASLIFSINPDLSYKKVIQILKDSIVY 641
PfSub1
PfSOPT
PfSOPT REELRHLSNRAYYHDMMNTFEDSLNQRK 552
PfSub1 LPSLKNMVAWAGYADINKAVNLAIKSKK 669
PfSub1

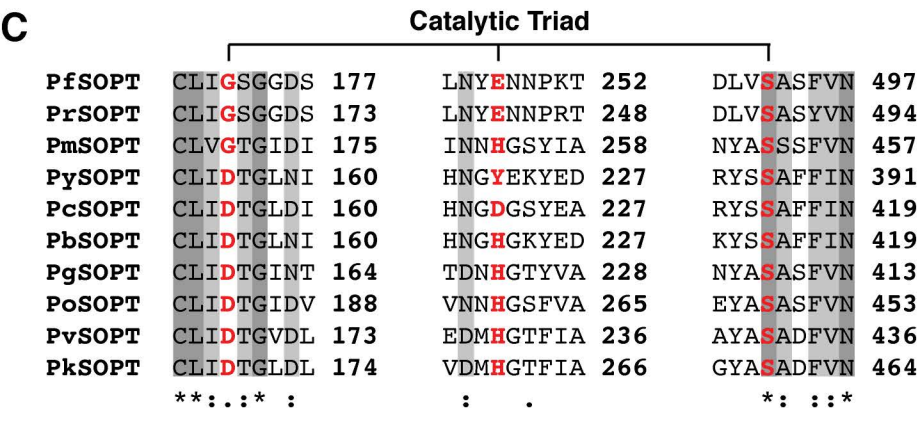
C
Catalytic Triad
PfSOPT CLIGSGGDS 177 LNYENNPKT 252 DLVSASFVN 497
PrSOPT CLIGSGGDS 173 LNYENNPRT 248 DLVSASYVN 494
PmSOPT CLVGTGIDI 175 INNHGSYIA 258 NYASSSFVN 457
PySOPT CLIDTGLNI 160 HNGYEKYED 227 RYSSAFFIN 391
PcSOPT CLIDTGLDI 160 HNGDGSYEA 227 RYSSAFFIN 419
PbSOPT CLIDTGLNI 160 HNGHGKYED 227 KYSSAFFIN 419
PgSOPT CLIDTGINT 164 TDNHGTYVA 228 NYASASFVN 413
PoSOPT CLIDTGIDV 188 VNNHGSFVA 265 EYASASFVN 453
PvSOPT CLIDTGVDL 173 EDMHGTFIA 236 AYASADFVN 436
PkSOPT CLIDTGLDL 174 VDMHGTFIA 266 GYASADFVN 464

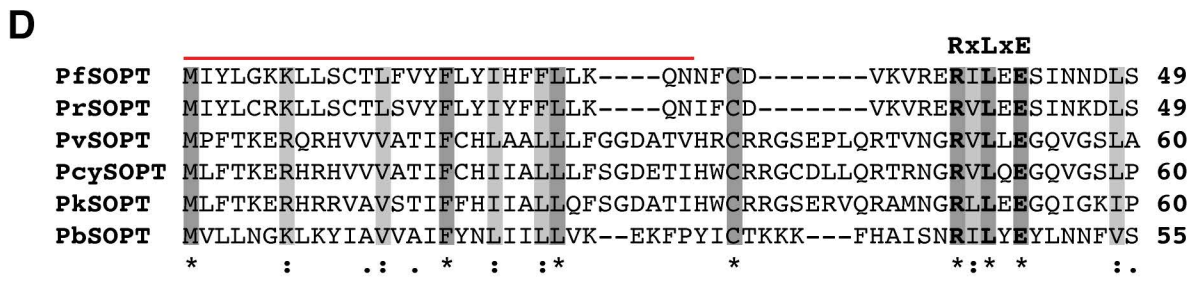
D
RxLxE
PfSOPT MIYLGKKLLSCTLFVYFLYIHFFLLK----QNNFCD-------VKVRERILEESINNDLS 49
PrSOPT MIYLCRKLLSCTLSVYFLYIYFFLLK----QNIFCD-------VKVRERVLEESINKDLS 49
PvSOPT MPFTKERQRHVVVATIFCHLAALLLFGGDATVHRCRRGSEPLQRTVNGRVLLEGQVGSLA 60
PcySOPT MLFTKERHRHVVVATIFCHIIALLLFSGDETIHWCRRGCDLLQRTRNGRVLQEGQVGSLP 60
PkSOPT MLFTKERHRRVAVSTIFFHIIALLQFSGDATIHWCRRGSERVQRAMNGRLLEEGQIGKIP 60
PbSOPT MVLLNGKLKYIAVVAIFYNLIILLVK--EKFPYICTKKK---FHAISNRILYEYLNNFVS 55


E
PfSOPT_1-62-GFP
Signal Peptide
RILEE
20 aa
GFP
MIYLGKKLLSCTLFVYFLYIHFFLLKQNNFC
DVKVRERILEESINNDLSSKGENLHIYEKTN - GFP

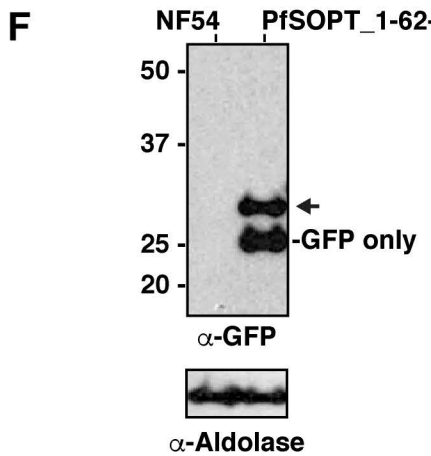
F
NF54
PfSOPT_1-62-GFP
50
37
25
20
-GFP only
α-GFP
α-Aldolase

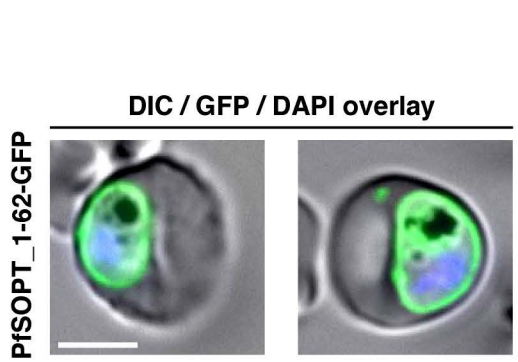
G
DIC / GFP / DAPI overlay
PfSOPT_1-62-GFP

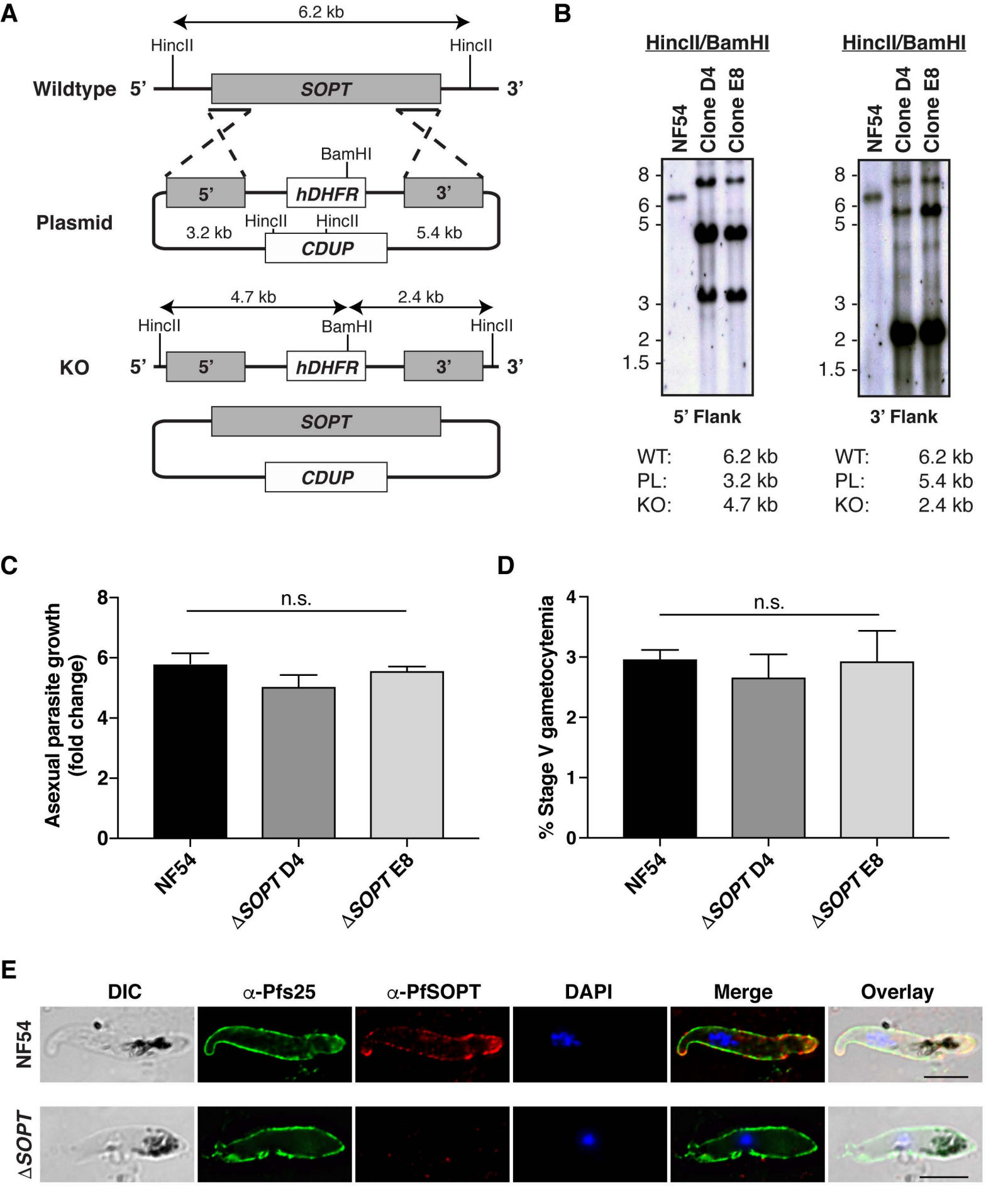
A
6.2 kb
HincII
HincII
Wildtype
5'
SOPT
3'
BamHI
5'
hDHFR
3'
Plasmid
3.2 kb
HincII
HincII
5.4 kb
CDUP
4.7 kb
2.4 kb
HincII
BamHI
HincII
KO
5'
5'
hDHFR
3'
3'
SOPT
CDUP
B
HincII/BamHI
HincII/BamHI
NF54
Clone D4
Clone E8
NF54
Clone D4
Clone E8
8
6
5
3
2
1.5
8
6
5
3
2
1.5
5' Flank
3' Flank
WT: 6.2 kb
PL: 3.2 kb
KO: 4.7 kb
WT: 6.2 kb
PL: 5.4 kb
KO: 2.4 kb
C
Asexual parasite growth (fold change)
n.s.
NF54
ΔSOPT D4
ΔSOPT E8
D
% Stage V gametocytemia
n.s.
NF54
ΔSOPT D4
ΔSOPT E8
E
DIC
α-Pfs25
α-PfSOPT
DAPI
Merge
Overlay
NF54
ΔSOPT

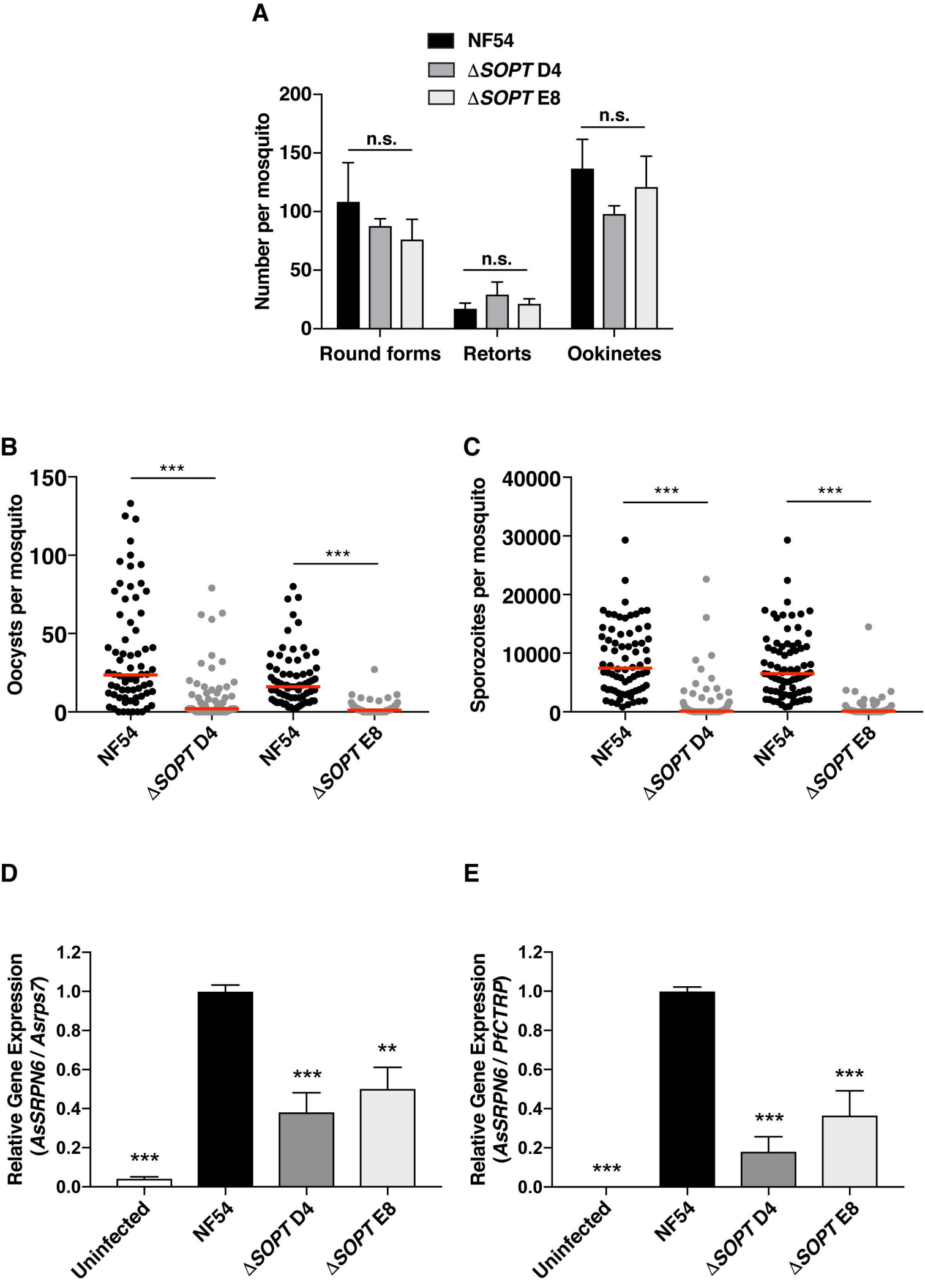
A
NF54
ΔSOPT D4
ΔSOPT E8
Number per mosquito
200
150
100
50
0
n.s.
n.s.
n.s.
Round forms
Retorts
Ookinetes
B
Oocysts per mosquito
150
100
50
0
***
***
NF54
ΔSOPT D4
NF54
ΔSOPT E8
C
Sporozoites per mosquito
40000
30000
20000
10000
0
***
***
NF54
ΔSOPT D4
NF54
ΔSOPT E8
D
Relative Gene Expression
(AsSRPN6 / Asrps7)
1.2
1.0
0.8
0.6
0.4
0.2
0.0
***
***
**
Uninfected
NF54
ΔSOPT D4
ΔSOPT E8
E
Relative Gene Expression
(AsSRPN6 / PfCTRP)
1.2
1.0
0.8
0.6
0.4
0.2
0.0
***
***
***
Uninfected
NF54
ΔSOPT D4
ΔSOPT E8

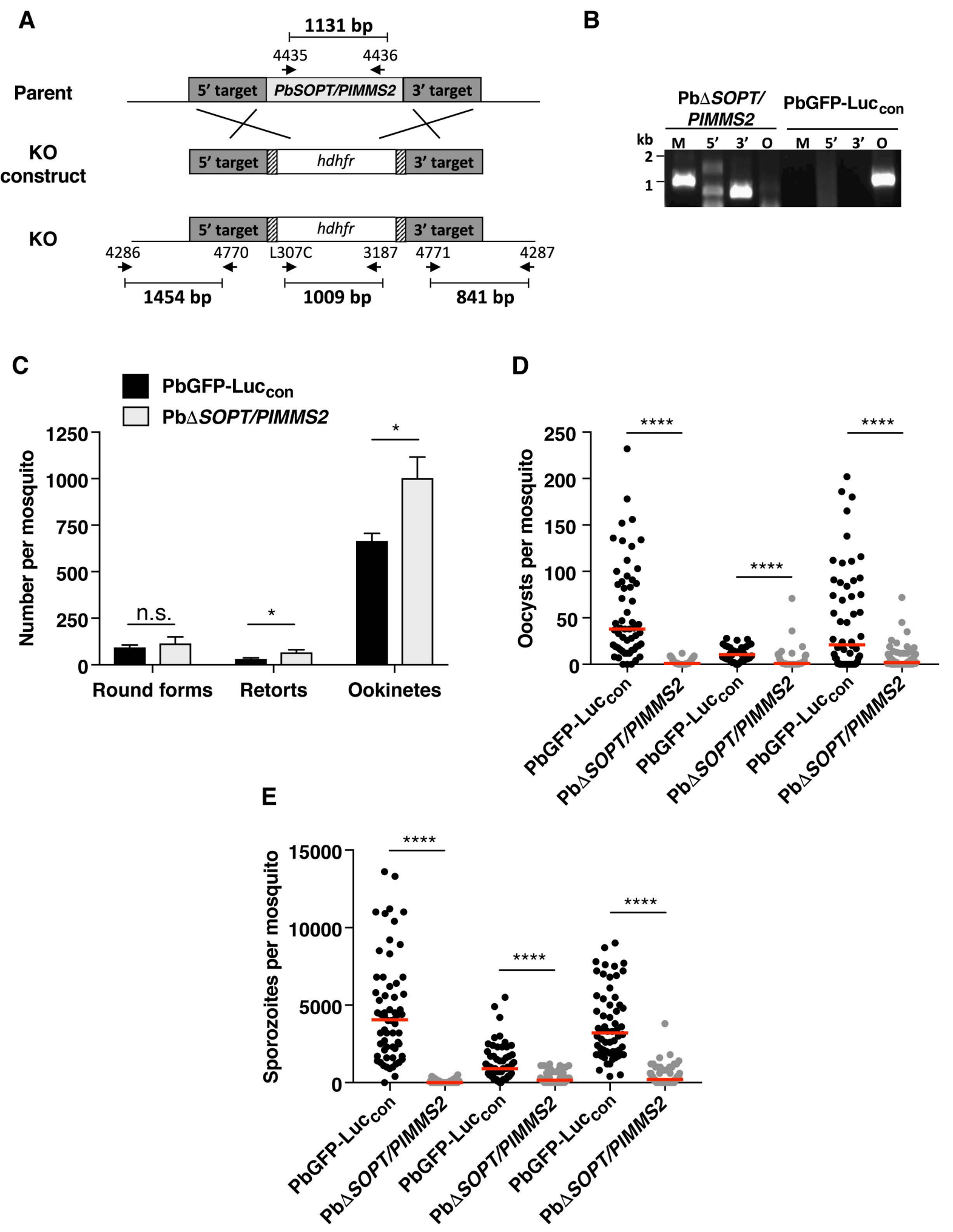
A
1131 bp
4435
4436
Parent
5' target
PbSOPT/PIMMS2
3' target
KO construct
5' target
hdhfr
3' target
KO
5' target
hdhfr
3' target
4286
4770
L307C
3187
4771
4287
1454 bp
1009 bp
841 bp
B
PbΔSOPT/PIMMS2
PbGFP-Luccon
kb
M
5'
3'
O
M
5'
3'
O
2
1
C
PbGFP-Luccon
PbΔSOPT/PIMMS2
Number per mosquito
1250
1000
750
500
250
0
n.s.
*
*
Round forms
Retorts
Ookinetes
D
Oocysts per mosquito
250
200
150
100
50
0
****
****
****
PbGFP-Luccon
PbΔSOPT/PIMMS2
PbGFP-Luccon
PbΔSOPT/PIMMS2
PbGFP-Luccon
PbΔSOPT/PIMMS2
E
Sporozoites per mosquito
15000
10000
5000
0
****
****
****
PbGFP-Luccon
PbΔSOPT/PIMMS2
PbGFP-Luccon
PbΔSOPT/PIMMS2
PbGFP-Luccon
PbΔSOPT/PIMMS2

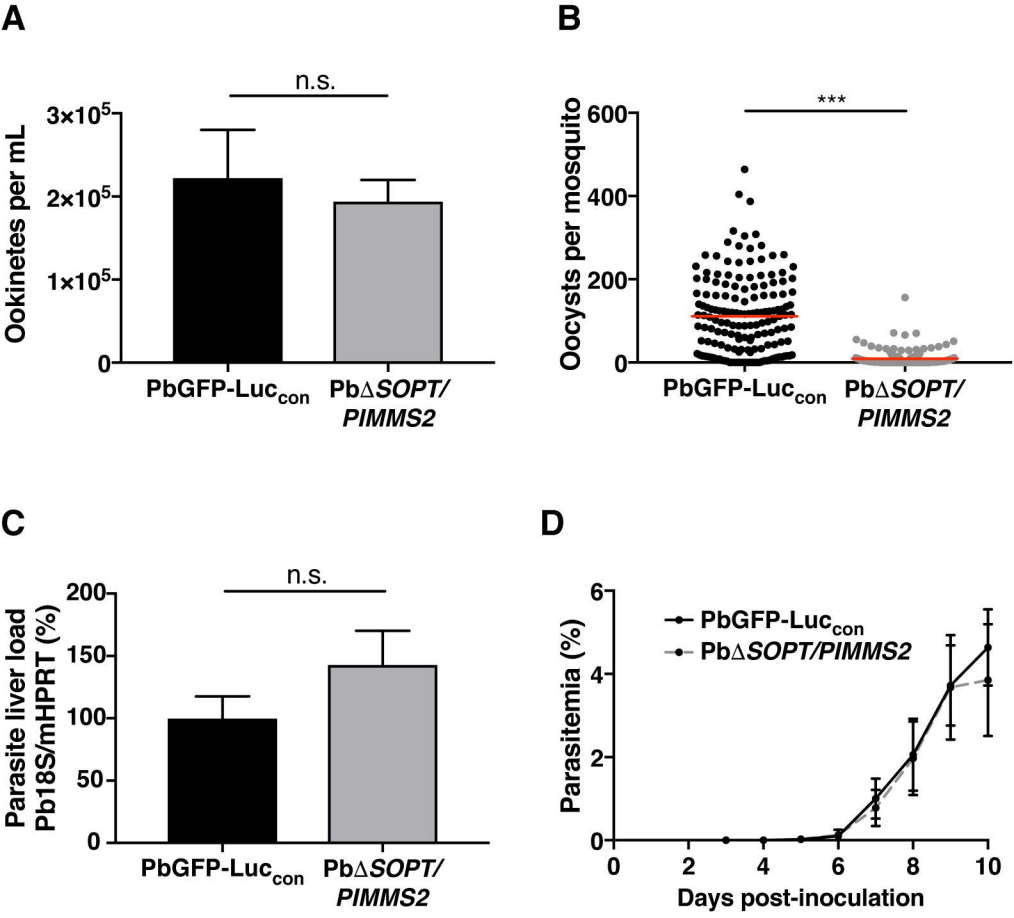
A
n.s.
3×10^5
2×10^5
1×10^5
0
Ookinetes per mL
PbGFP-Luc_con
PbΔSOPT/PIMMS2
B
***
600
400
200
0
Oocysts per mosquito
PbGFP-Luc_con
PbΔSOPT/PIMMS2
C
n.s.
200
150
100
50
0
Parasite liver load Pb18S/mHPRT (%)
PbGFP-Luc_con
PbΔSOPT/PIMMS2
D
PbGFP-Luc_con
PbΔSOPT/PIMMS2
6
4
2
0
Parasitemia (%)
0
2
4
6
8
10
Days post-inoculation

Table S1. *P. falciparum* transmission to *An. stephensi* in standard membrane feeding assays.

	Oocysts			Sporozoites		
		PfΔ*SOPT*			PfΔ*SOPT*	
	NF54	**D4**	**E8**	**NF54**	**D4**	**E8**
Experiment 1						
N	19	22	21	29	24	28
Range	2-72	0-6	0-9	800-29300	0-800	0-300
Mean	25	0.95	0.86	9817	163	68
Median	18	0	0	7900	100	0
Prevalence	1	0.41	0.29	1	0.54	0.39
% Inhibition, prevalence		59	71		46	61
% Inhibition, intensity		100	100		98.7	100
Mann-Whitney U		5	6.5		0.5	0
P value		<0.0001	<0.0001		<0.0001	<0.0001
Experiment 2						
N	31	33	n.d.	20	20	n.d.
Range	0-133	0-79		1400-17300	0-22600	
Mean	48	17		8580	5160	
Median	37	10		7750	3450	
Prevalence	0.81	0.88		1	0.95	
% Inhibition, prevalence		-8.6			0.05	
% Inhibition, intensity		72.9			55.5	
Mann-Whitney U		354			121	
P value		0.033			0.0309	
Experiment 3						
N	32	n.d.	26	25	n.d.	25
Range	2-52		0-11	933-16533		0-14467
Mean	13		2.3	5653		1624
Median	9.5		1.5	5333		1067
Prevalence	1		0.73	1		0.88
% Inhibition, prevalence			27			12
% Inhibition, intensity			84.2			80
Mann-Whitney U			66			63
P value			<0.0001			<0.0001
Experiment 4						
N	20	20	20	23	31	24
Range	9-80	0-14	0-27	1200-16700	0-1600	0-3700
Mean	29	3.2	4	7852	223	554
Median	24	0.5	1.5	6800	0	50
Prevalence	1	0.5	0.6	1	0.29	0.5
% Inhibition, prevalence		50	40		71	50
% Inhibition, intensity		98.7	93.8		100	99.3
Mann-Whitney U		6	15		3.5	11
P value		<0.0001	<0.0001		<0.0001	<0.0001

n.d., not done

Table S2. Transmission of *P. berghei* to *An. stephensi* in direct feeding assays.

	Oocysts		Sporozoites	
	PbGFP-luc$_{con}$	**Pb△*SOPT/PIMMS2***	**PbGFP-luc$_{con}$**	**Pb△*SOPT/PIMMS2***
Experiment 1				
N	56	64	62	60
Range	0-232	0-12	0-13600	0-500
Mean	56.52	2.719	4623	85
Median	38	1	4050	0
Prevalence	0.95	0.69	0.98	0.43
% Inhibition, prevalence		27.4		56.1
% Inhibition, intensity		97.4		100
Mann-Whitney U		202		
P value		<0.0001		
Experiment 2				
N	36	42	61	60
Range	0-28	0-71	0-5500	0-1200
Mean	11.92	5.333	1249	308.3
Median	10.5	1	900	150
Prevalence	0.95	0.6	0.97	0.56
% Inhibition, prevalence		36.8		42.3
% Inhibition, intensity		90.5		83.3
Mann-Whitney U		284		
P value		<0.0001		
Experiment 3				
N	56	76	60	57
Range	0-202	0-72	0-9000	0-3800
Mean	45.86	6.211	3743	475.4
Median	21	2	3200	200
Prevalence	0.75	0.65	1	0.59
% Inhibition, prevalence		13.3		41
% Inhibition, intensity		90.5		93.8
Mann-Whitney U		1192		
P value		<0.0001		

Table S3. Transmission of *P. berghei* ookinetes to *An. stephensi* in standard membrane feeding assays.

	PbGFP-luc$_{con}$	Pb△*SOPT/PIMMS2*
Experiment 1		
N	51	45
Range	0-464	0-70
Mean	139.2	17.42
Median	114	14
Prevalence	0.88	0.93
% Inhibition, prevalence		-5.68
% Inhibition, intensity		87.7
Mann-Whitney U		366.5
P value		< 0.0001
Experiment 2		
N	51	24
Range	0-316	1-156
Mean	151	26.08
Median	136	13.5
Prevalence	0.92	1
% Inhibition, prevalence		-8.7
% Inhibition, intensity		90.1
Mann-Whitney U		124.5
P value		<0.0001
Experiment 3		
N	30	45
Range	0-192	0-1
Mean	54.6	0.089
Median	33.5	0
Prevalence	0.96	0.09
% Inhibition, prevalence		90.6
% Inhibition, intensity		100
Mann-Whitney U		24.5
P value		< 0.0001
Experiment 4		
N	30	47
Range	0-204	0-8
Mean	52.5	1.7
Median	27.5	1
Prevalence	0.93	0.617
% Inhibition, prevalence		33.7
% Inhibition, intensity		96.4
Mann-Whitney U		113.5
P value		< 0.0001

Table S4. Oligonucleotides used in this study.

Oligo	Description	5'-3' sequence
mo430	PFE0360c knockout 5' flank	atcccgcggTAGATCCAAGAATATGGCCAAATTGG
mo431		gatactagtGATCCGATTAAACACACTTTGG
mo432	PFE0360c knockout 3' flank	atatcctaggGTAGAGCAGGAAACAAGTGTGG
mo433		tccggcgccCTTTGGAGAATTGCGTGTTCC
JB135	PFE0360c -Glux 3' flank	cagctcgagGACATTTGTCTAATAGGGCA
JB136		atccccgggTCGTTTAAATTTTATCTTTGGA
JB160	PFE0360c -HA 3' flank	atcagatctTAAGGTATTGTTATCTGATG
JB161		atcctgcaggTCGTTTAAATTTTATCTTTGG
JB32	PFE0360c -Glux GFP reverse	acaactccagtgaaaagtt
JB51	PFE0360c -Glux CRT-5'UTR of plasmid	gactataatatccgttaat
DT-R	PFE0360c -HA PbDT3' reverse	CAgTTATAAATACAATCAATT
JB101	PFE0360c- HA Detect integration of 3' HA tag	CCATGATTACGCCAAGCTAT
mo434	sense oligo that binds upstream of 5'flank for detection of 5' integration event	tacagaccccgttggtgg
mo435	antisense oligo that binds downstream of 3'Flank for detection of 3' integration event	cacatttttctagtcttcaaagg
SL192	As_SRPN6 sense oligo for RT-qPCR	ACTACGACGATGTCCCGAAC
SL193	As_SRPN6 antisense oligo for RT-qPCR	ATCGATCGGTTGTACCAAGG
JB207	As_rps7 sense oligo for RT-qPCR	TGCGGCTTCAGATCCGAGTTC
JB208	As_rps7 antisense oligo for RT-qPCR	TTCGTTGTGAACCCAAATAAAAATC
SL139	Pf_CTRP sense oligo for RT-qPCR	GAATGGAGTCCCTGTCCTGA

SL140	Pf_CTRP antisense oligo for RT-qPCR	TGGTCCTTTCCTTTCCCTTT
PR92	Pb_18S sense oligo for RT-qPCR	GGAGATTGGTTTTGACGTTTATGTG
PR93	Pb_18S antisense oligo for RT-qPCR	AAGCATTAAATAAAGCGAATACATCCTTAC
PR94	mHPRT sense oligo for RT-qPCR	CATTATGCCGAGGATTTGGA
PR95	mHPRT antisense oligo for RT-qPCR	AATCCAGCAGGTCAGCAAAG
4744	5'UTR-F	GAACTCGTACTCCTTGGTGACGGGTACCGTTACAACGTTGTAAAATTGTCC
4745	5'UTR-R	CATCTACAAGCATCGTCGACCTCGTGTCTATTAAGCATACTGAGG
4746	3'UTR-F	CCTTCAATTTCGGATCCACTAGTATGAAGATAATAAACGAGGTAG
4747	3'UTR-R	AGGTTGGTCATTGACACTCAGCAGTACTCTACTAATTTTGAGGTATAACTC
4661	Primer Tag (5'UTR end)	GAACTCGTACTCCTTGGTGACG
4662	Primer Tag (3'UTR end)	AGGTTGGTCATTGACACTCAGC
4286	5'-integ.-F	CATAGAATTTGATCAGAGAGCC
4770	pL0040 SM 5UTR region R-Tag (SM+5_R_Tag)	CATCTACAAGCATCGTCGACCTC
4771	pL0040 SM 3UTR region F-Tag (SM+3_F_Tag)	CCTTCAATTTCGGATCCACTAG
4287	3'-integ.-R	TATGATTATTCTATGTTTGGGC
L307C	*hdhfr F*	GCTTAATTCTTTTCGAGCTC
3187	*hdhfr R*	GTGTCACTTTCAAAGTCTTGC
4435	orf	CAGTATGCTTAATAGACACTGG
4436	orf	TCATCAGAACCACCTTCGTC

Figure. S1

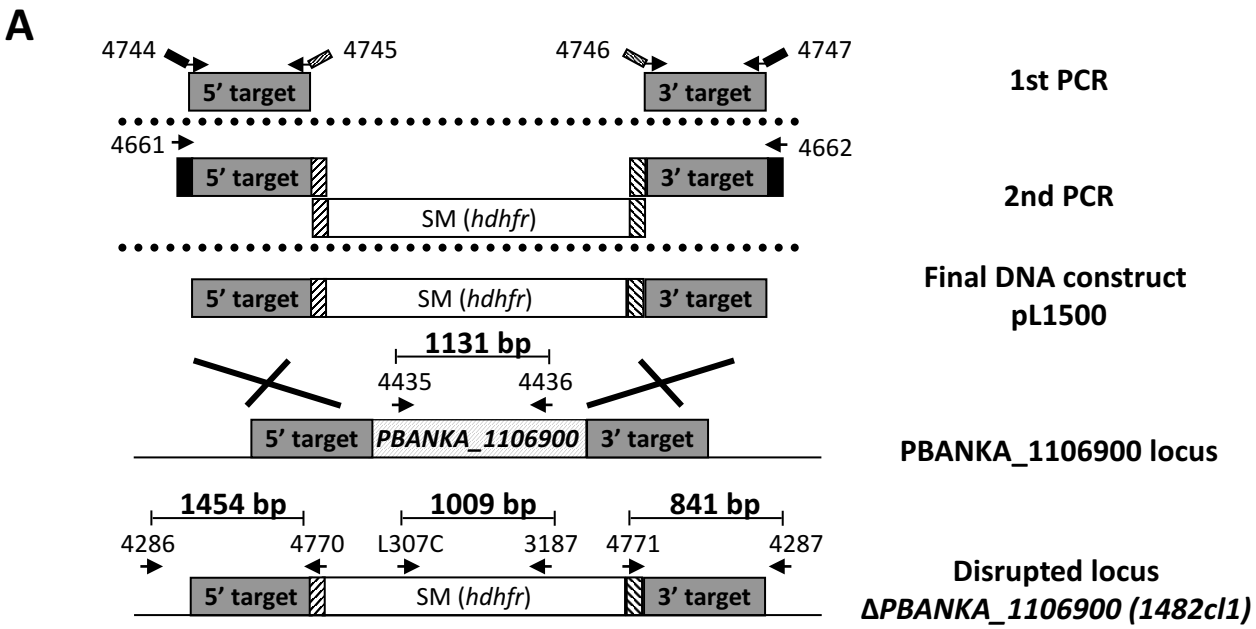
A
4744
4745
4746
4747
5' target
3' target
1st PCR
4661
4662
SM (hdhfr)
2nd PCR
Final DNA construct
pL1500
1131 bp
4435
4436
PBANKA_1106900
PBANKA_1106900 locus
1454 bp
1009 bp
841 bp
4286
4770
L307C
3187
4771
4287
Disrupted locus
ΔPBANKA_1106900 (1482cl1)

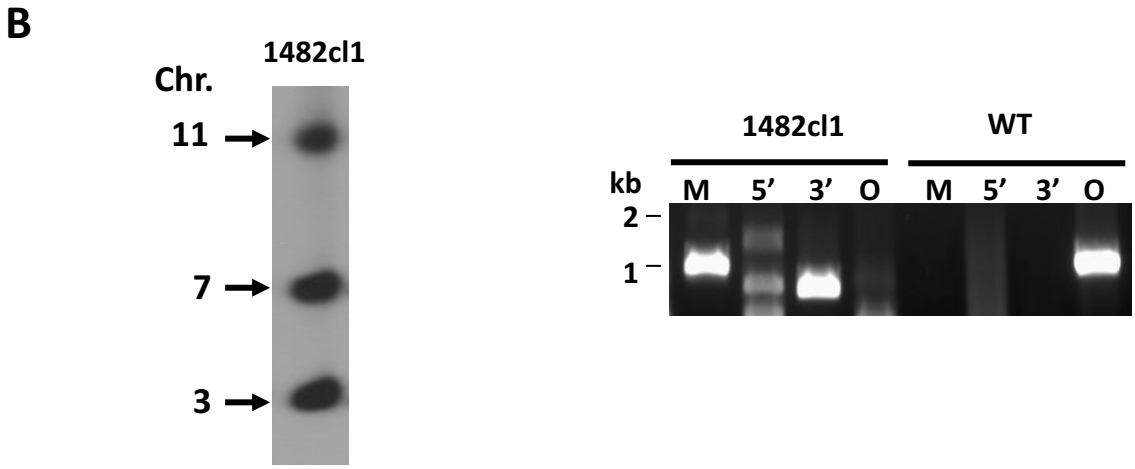
B
1482cl1
Chr.
11
7
3
1482cl1
WT
kb
M
5'
3'
O
2
1